AMaPO: Adaptive Margin-attached Preference Optimization for Language Model Alignment

Ruibo Deng^{1,2}, Duanyu Feng^{1,2}, Wenqiang Lei^{1,2}*

¹Sichuan University, Chengdu, China ²Engineering Research Center of Machine Learning and Industry Intelligence, Ministry of Education, China dengruibo@stu.scu.edu.cn, fengduanyuscu@stu.scu.edu.cn, wenqianglei@scu.edu.cn

Abstract

Offline preference optimization offers a simpler and more stable alternative to RLHF for aligning language models. However, their effectiveness is critically dependent on ranking accuracy, a metric where further gains are highly impactful. This limitation arises from a fundamental problem that we identify and formalize as the Overfitting-Underfitting Dilemma: current margin designs cause models to apply excessive, wasteful gradients to correctly ranked samples (overfitting) while providing insufficient corrective signals for misranked ones (underfitting). To resolve this dilemma, we propose Adaptive Margin-attached Preference Optimization (AMaPO), a simple yet principled algorithm. AMaPO employs an instance-wise adaptive margin, refined by Znormalization and exponential scaling, which dynamically reallocates learning effort by amplifying gradients for misranked samples and suppressing them for correct ones. Extensive experiments on widely used benchmarks demonstrate that AMaPO not only achieves better ranking accuracy and superior downstream alignment performance, but targeted analysis also confirms that it successfully mitigates the core overfitting and underfitting issues. 1

1 Introduction

Aligning Large Language Models (LLMs) with human preferences, ensuring they are helpful, honest, and harmless, also known as preference learning, is crucial for LLM research (Bai et al. 2022; Ouyang et al. 2022). A standard approach for this task is Reinforcement Learning from Human Feedback (RLHF), a powerful online algorithm that first trains a reward model on human preferences and then uses reinforcement learning to optimize the LLMs (Ouyang et al. 2022; Schulman et al. 2017). Despite its demonstrated success, RLHF is notoriously complex and prone to training instabilities, presenting significant practical challenges (Engstrom et al. 2020). To circumvent these issues, a new family of offline alignment algorithms has emerged, led by methods like DPO (Rafailov et al. 2023), IPO (Azar et al. 2024), KTO (Ethayarajh et al. 2024) and FocalPO (Liu et al. 2025). These approaches offer superior simplicity and sta-

*Corresponding author

Copyright © 2026, Association for the Advancement of Artificial Intelligence (www.aaai.org). All rights reserved.

¹Our code: https://github.com/Shiroha-Offical/AMaPO

bility by directly optimizing the LLMs to favor preferred responses over dispreferred ones, thereby bypassing the need for an explicit reward model and the complexities of RL. At its core, the efficacy of this entire paradigm is the ranking accuracy of an implicit reward model, which dictates how well the optimization process can distinguish between desirable and undesirable outputs.

Therefore, many subsequent DPO-style methods have been used to improve ranking accuracy, either explicitly prioritizing ranking (Chen et al. 2024) or indirectly fostering this capability through other modifications. A primary direction of these methods is to manipulate the implicit reward function, often by incorporating a reward margin to better separate preferred and dispreferred responses. Innovations in this direction include introducing fixed or dynamic margins (Meng, Xia, and Chen 2024; Wu et al. 2024) or updating the reference model to create more favorable optimization landscapes (Gorbatovski et al. 2024). Although these methods report improved performance, their contributions are typically validated empirically, without a unified theoretical perspective to explain how these methods dynamically affect ranking accuracy during training and to compare with each others. Separately, emerging work has analyzed the gradient dynamics of preference learning algorithms (Feng et al. 2024; Yan et al. 2024; Yuan et al. 2024; Ma et al. 2025). However, these studies often fail to explicitly connect their findings on gradient properties, such as magnitude or conflict, with the resulting changes in ranking accuracy. Therefore, we argue that a crucial analytical bridge is missing: a framework that not only examines the gradient dynamics of these advanced DPO variants but also directly links them to the dynamic evolution of ranking accuracy.

To bridge this analytical gap, we introduce a unified framework that analyzes DPO-style methods through the lens of the reward margin. First, we reformulate existing algorithms, including DPO and its variants, into a generalized objective function based on different margin designs. This unification establishes a direct, formal connection between the algorithmic structure of each method and its capacity to optimize ranking accuracy. Within this framework, we then employ gradient dynamics analysis to investigate how these distinct margin formulations shape the learning trajectory of ranking accuracy. Our analysis reveals a fundamental flaw in the standard DPO mechanism: for samples that are already

correctly ranked, its margin design leads to *overfitting* by assigning excessively large gradients, wasting capacity on these easy samples. Conversely, for incorrectly ranked samples where learning is most critical, the margin often results in *underfitting* by providing insufficient gradients, thereby hindering the correction of errors. We also find that while some of subsequent DPO-style methods attempt to address this, they fail to fully resolve this core tension.

Motivated by our analysis, we introduce AMaPO, an algorithm designed to resolve this overfitting-underfitting dilemma. AMaPO's core strategy is an instance-wise adaptive margin, refined by Z-normalization and exponential scaling. By dynamically assigning large corrective margins to underfit samples and a zero margin to correctly ranked ones, it effectively reallocates learning effort to where it is most needed. Our extensive experiments on diverse benchmarks demonstrate that AMaPO not only achieves state-of-the-art ranking accuracy and superior downstream alignment performance, but targeted analysis also confirms that it successfully mitigates the core overfitting and underfitting issues, validating our approach.

The main contributions of this paper are: (i) We introduce a unified margin-based framework to analyze gradient dynamics of DPO-style algorithms, which reveals an overfitting-underfitting dilemma: existing methods expend excessive gradient on already-learned preferences (overfitting) while providing insufficient signal to correct misranked ones (underfitting). (ii) We propose Adaptive Margin-attached Preference Optimization (AMaPO), a principled algorithm designed to resolve this dilemma. AMaPO employs an instance-wise adaptive margin and refined by Z-normalization and exponential scaling, that reallocates learning effort by amplifying gradients for misranked samples and suppressing them for correctly ranked ones. (iii) Extensive experiments demonstrate AMaPO achieves state-of-the-art ranking accuracy, solving the overfittingunderfitting dilemma and leading to superior downstream alignment performance like instruction-following and complex reasoning.

2 Related works

Preference Learning Algorithms The field of preference learning for LLM alignment is dominated by two primary approaches: online and offline. Online methods, exemplified by Reinforcement Learning from Human Feedback (RLHF) (Bai et al. 2022; Ouyang et al. 2022), employ a complex two-stage process of reward modeling and RL-based optimization. Offline methods, initiated by Direct Preference Optimization (DPO) (Rafailov et al. 2023), directly optimize the LLM on preference data, obviating practical challenges such as the need for a separate reward model and training instability. Optimized DPO variants generally fall into two categories: reformulating the core loss function (Azar et al. 2024; Ethayarajh et al. 2024), or incorporating an explicit reward margin to separate preference pairs robustly (Boser, Guyon, and Vapnik 1992; Turner and Firth 2012). This margin-based approach has been realized through employing fixed or instance-dependent margins to improve learning stability and handle potential data noise (Meng, Xia, and

Chen 2024; Kim et al. 2024; Amini, Vieira, and Cotterell 2024). Others achieve a form of dynamic regularization by progressively updating the reference policy itself, which effectively creates an adaptive margin throughout the training process (Gorbatovski et al. 2024; Wu et al. 2024). Despite these diverse, the central mechanism common to all these DPO-style algorithms is the implicit reward function. This makes their ability to learn to classify preferences correctly, known as the ranking accuracy (Chen et al. 2024), the paramount determinant of their success. However, the field currently lacks a unified framework to analyze how these different methods impact the evolution of ranking accuracy, leaving a critical gap in our understanding.

Preference Learning Theory Concurrent with the development of preference learning algorithms, a body of theoretical work has emerged to analyze their underlying mechanisms. These inquiries generally follow two primary perspectives: gradient dynamics and divergence analysis. From the gradient perspective, for example, (Feng et al. 2024) reveals the limited learning capacity of DPO through field theory and (Yuan et al. 2024) identify issues such as gradient entanglement in margin-based methods. From divergence perspective, it examines how DPO optimizes the model distribution π_{θ} towards the distribution of chosen response. While DPO implicitly optimizes a forward KL-divergence, recent work identifies promoting mode-seeking behavior by optimizing a reverse KL-divergence or Total Variation distance as a crucial property for preference alignment(Tajwar et al. 2024; Xiao et al. 2024, 2025). While these analyses are foundational, they typically examine each algorithm as a distinct entity. In this paper, we also want to build upon the tradition of gradient analysis but introduce a novel, unifying perspective. Based on the unification, we further explicitly connect the specific gradient properties of each method to their dynamic impact on ranking accuracy.

3 Preliminaries

This section establishes the technical foundations for our analysis. First, we detail Direct Preference Optimization (DPO) (Rafailov et al. 2023), the seminal algorithm for offline preference learning that serves as the basis for the methods we investigate. Second, we formalize the concept of the reward margin, which is used to construct a unified representation of various DPO-style algorithms. Finally, we define ranking accuracy, the primary metric used throughout our work to evaluate the efficacy of these alignment methods.

3.1 Direct Preference Optimization

Preference Data and the Bradley-Terry Model. Offline preference optimization relies on a static dataset of preferences, $\mathcal{D} = \{(x^{(i)}, y_w^{(i)}, y_l^{(i)})\}_{i=1}^N$. Each entry consists of a prompt $x^{(i)}$ and a pair of responses, $(y_w^{(i)}, y_l^{(i)})$, where y_w is preferred over y_l , denoted as $y_w \succ y_l$. This preference is typically provided by a human annotator or a powerful reward model. A standard assumption in the field is that these preferences are drawn from a distribution that follows the Bradley-Terry (BT) model (Bradley and Terry 1952), which

models the probability of preferring y_w over y_l as a logistic function of the difference in their latent reward values: $p(y_w \succ y_l|x) = \sigma(r(x, y_w) - r(x, y_l))$.

The Direct Preference Optimization. Instead of explicitly training a reward model r(x,y), Direct Preference Optimization (DPO) (Rafailov et al. 2023) derives an analytical mapping from the optimal policy to the reward function. This allows DPO to use the log-likelihood of the policy to implicitly represent the reward function via a closed-form expression with the optimal policy:

$$\mathcal{L}_{\text{DPO}}(\pi_{\theta}; \mathcal{D}) = -\mathbb{E}_{(x, y_w, y_l) \sim \mathcal{D}} \left[\log \sigma \left(\beta \log \frac{\pi_{\theta}(y_w | x)}{\pi_{\text{ref}}(y_w | x)} - \beta \log \frac{\pi_{\theta}(y_l | x)}{\pi_{\text{ref}}(y_l | x)} \right) \right], \tag{1}$$

where $\pi_{\rm ref}$ is a fixed reference model, and β is a temperature parameter that scales the reward.

3.2 A Unified Margin-based Framework

Recent theoretical works have sought to unify DPO-style algorithms under a single mathematical representation (Yuan et al. 2024; Liu, Liu, and Cohan 2024). A common approach is to formulate a general loss function that captures variations in reward shaping and regularization. However, with the increasing prominence of methods that explicitly engineer a reward margin (Zhao et al. 2024; Wu et al. 2024), these existing frameworks can represent such methods only indirectly, obscuring the margin's central role.

To create a more direct analytical tool that reflects this research trend, we extend the prior work (Yuan et al. 2024) by proposing a refined unified objective with the margin, γ :

$$\mathcal{L}_{\text{unified}}(\theta) = -\left(m(h_w(\log \pi_w) - h_l(\log \pi_l) - \gamma\right) + \Lambda(\log \pi_w). \tag{2}$$

Here, $h_w(x)$ and $h_l(x)$ represent transformation or adjustment functions applied to the log-probabilities of the preferred and dispreferred responses, respectively. π_w and π_l represent $\pi_\theta\left(y_w|x\right)$ and $\pi_\theta\left(y_l|x\right)$ for simplicity, respectively. The term m(x) is a scoring function that computes the difference between these transformed values with the margin γ . Finally, $\Lambda\left(\log\pi_w\right)$ is an optional auxiliary term that some models incorporate to encourage additional learning specifically on the preferred response. This formulation allows us to directly compare algorithms based on their margin design. For instance:

DPO: The original DPO algorithm fits this framework with $h_w(x) = h_l(x) = \beta x$, $m(x) = \log \sigma(x)$ and a fixed margin of $\gamma = \beta(\log \pi_{\mathrm{ref}}(y_w|x) - \log \pi_{\mathrm{ref}}(y_l|x))$.

SimPO: Simple Preference Optimization (SimPO) (Meng, Xia, and Chen 2024) is a highly effective DPO variant, shown as

$$\mathcal{L}_{\text{SimPO}}(\pi_{\theta}; \mathcal{D}) = -\mathbb{E}_{(x, y_w, y_l) \sim \mathcal{D}} \left[\log \sigma \left(\frac{\beta}{|y_w|} \log \pi_{\theta} \left(y_w | x \right) - \frac{\beta}{|y_l|} \log \pi_{\theta} \left(y_l | x \right) - C \right) \right]. \tag{3}$$

It fits our framework by defining $h_w(x) = \frac{\beta}{|y_w|} x$, $h_l(x) = \frac{\beta}{|y_w|} x$, $m(x) = \log \sigma(x)$ and a tunable margin $\gamma = C > 0$.

This margin-focused unification serves as the cornerstone of our gradient analysis. ²

3.3 Ranking Accuracy

While the ultimate goal of alignment is to produce generations that humans prefer, which is often evaluated by winrate against a baseline model (Zheng et al. 2023b), this metric is costly and ill-suited for tracking training dynamics. Therefore, a more direct and practical metric is crucial for analyzing the learning process. Ranking accuracy (Liu et al. 2024; Chen et al. 2024) directly measures whether the policy (training) model π_{θ} itself assigns a higher likelihood to the preferred response over the dispreferred one for a given prompt. Formally, it is defined as:

$$\mathcal{R}(\pi_{\theta}; \mathcal{D}) = \frac{1}{|\mathcal{D}|} \sum_{(x, y_w, y_l) \in \mathcal{D}} \mathbb{I}\left[\pi_{\theta}(y_w|x) > \pi_{\theta}(y_l|x)\right], \tag{4}$$

where $\mathbb{I}[\cdot]$ is the indicator function. A higher ranking accuracy indicates that the policy's preference ordering aligns with the ground-truth data, and it serves as a predictor of the downstream performance within a certain KL divergence range (Chen et al. 2024). Furthermore, for our theoretical analysis, we utilize the instance-wise ranking accuracy derived from our unified framework (Eq. 2), defined as $h_w(\log \pi_w) - h_l(\log \pi_l)$. For the vast majority of DPO-style methods where the transformations h_w and h_l are linear or monotonic, the sign of this score is equivalent to the standard ranking accuracy (i.e., $h_w(\log \pi_w) - h_l(\log \pi_l) > 0 \iff \pi_\theta(y_w|x) > \pi_\theta(y_l|x)$). Throughout this paper, we use this ranking accuracy as the primary lens for analysis.

4 Methods

In this section, we leverage the unified margin-based framework established in the previous section to conduct a detailed theoretical analysis and construct our related method. Our primary goal is to understand how the margin design in DPO and its variants affects the learning dynamics of ranking accuracy. Through this gradient-level investigation, we diagnose the key limitations of existing approaches and, from these findings, distill a set of desiderata for a more effective margin function. Building on these principles, we then introduce **Adaptive Margin-attached Preference Optimization (AMaPO)**, a novel preference optimization algorithm that assigns an adaptive margin specifically designed to manipulate gradient magnitude, thereby improving both ranking accuracy and overall alignment performance.

4.1 Gradient Dynamics and the Ideal Margin

Based on the unified objective in Eq. 2, we can derive a general gradient formulation for DPO-style algorithms. The gradient with respect to the model parameters θ is:

$$\nabla_{\boldsymbol{\theta}} \mathcal{L}_{\text{unified}}(\boldsymbol{\theta}) = -m'(h_w(\log \pi_w) - h_l(\log \pi_l) - \gamma)$$
$$(h'_w(\log \pi_w) - h'_l(\log \pi_l)) - \Lambda'(\log \pi_w). \quad (5)$$

²For completeness, we formulate other common DPO-style methods within this framework in Appendix B.1.

Table 1: All four possible cases for training dynamics of the unified framework in Eq. 2, where \uparrow and \downarrow indicate increase and decrease, $r_{\pi_{\theta}}(x, y_w, y_l) = h_w(\log \pi_w) - h_l(\log \pi_l)$. The **correctly ranked** means $r_{\pi_{\theta}}(x, y_w, y_l) > 0$, the **incorrectly ranked** means $r_{\pi_{\theta}}(x, y_w, y_l) \leq 0$. **Case 1** and **Case 4** are the ideal behavior which properly control the learning rate.

Case	$r_{\pi_{\theta}}(x, y_w, y_l), \gamma$	$ d_{\boldsymbol{\theta}} $	Influence
1	$r_{\pi_{\theta}}(x, y_w, y_l) \ge \gamma$	\downarrow	mild update on correctly ranked samples, ideal.
2	$r_{\pi_{\theta}}(x, y_w, y_l) < \gamma$	↑	aggressive update on correctly ranked samples, overfitting.
3	$r_{\pi_{\theta}}(x, y_w, y_l) \ge \gamma$	+	mild update on incorrectly ranked samples, underfitting.
4	$r_{\pi_{\theta}}(x, y_w, y_l) < \gamma$		aggressive update on incorrectly ranked samples, ideal.

Specifically, we define $d_{\theta} = m'(h_w(\log \pi_w) - h_l(\log \pi_l) - \gamma)$, which comprises log-probabilities of responses $(h_w(\log \pi_w), h_l(\log \pi_l))$ and margin γ and significantly affects the gradient magnitude³.

This insight reveals a crucial mechanism: for a given state of the policy π_{θ} , the margin γ is the primary lever to control the learning rate. Since the gradient magnitude d_{θ} is governed by

$$d_{\theta} = m'(h_w(\log \pi_w) - h_l(\log \pi_l) - \gamma) \tag{6}$$

where m' is usually a monotonically decreasing function and m'(x) > 0 (as $m(x) = \log \sigma(x)$), the choice of γ directly determines whether the learning signal is amplified or suppressed. A poorly designed margin leads directly to what we term the Overfitting-Underfitting Dilemma.

Definition 1 (The Overfitting-Underfitting Dilemma) An algorithm is susceptible to this dilemma when its margin γ causes inefficient optimization:

- Overfitting: A large margin produces wasteful gradients for correctly ranked samples, forcing the model to overoptimize on these samples.
- Underfitting: A small margin yields small gradients for incorrectly ranked samples, stifling learning where it is most needed.

Table 1 provides a concrete illustration of these cases. Resolving this dilemma requires a margin that adheres to a key principle: it must be **dynamically adaptive** to the policy's instance-wise ranking accuracy. This motivates the concept of an Oracle Ranking Margin.

Definition 2 (Oracle Ranking Margin) The **Oracle Ranking Margin**, γ^* , is an instance-specific, non-negative threshold that acts as a dynamic learning target ⁴, distinguishing between incorrectly ranked samples that require a strong learning signal $r_{\pi_{\theta}}(x, y_w, y_l) < \gamma^*$, and correctly ranked ones whose gradients should be suppressed to prevent overfitting $r_{\pi_{\theta}}(x, y_w, y_l) > \gamma^*$. The instance-wise ranking accuracy $r_{\pi_{\theta}}(x, y_w, y_l)$ is defined as $h_w(\log \pi_w) - h_l(\log \pi_l)$.

With these principles established, to thoroughly investigate whether existing DPO-style algorithms satisfy the above demands, our analysis focuses on two of the most celebrated objectives, including DPO and SimPO ⁵.

Analysis of DPO. The margin, $\gamma = \beta \log \pi_{\rm ref}(y_w|x) - \beta \log \pi_{\rm ref}(y_l|x)$ derived from the reference model, can neither dynamically adapt to instance-wise ranking correctness nor remaining positive. This irrelevance suggests that DPO can reproduce all cases above, which might result in overfitting and underfitting, as illustrated by case 2 and case 3.

Analysis of SimPO. Although $\gamma=C>0$ is guaranteed to remain positive, it overlooks the variability inherent in instance-wise ranking correctness. This rigidity suggests that SimPO can reproduce case 2 and case 4, which could lead to overfitting as shown in case 2.

Our analysis reveals that margin designs of both DPO and SimPO fail to proactively adapt based on instance-wise ranking correctness, leading to overfitting and underfitting in preference learning and, consequently, suboptimal ranking accuracy and alignment performance.

4.2 AMaPO: Adaptive Margin-attached Preference Optimization

To overcome the aforementioned limitations, we introduce **Adaptive Margin-attached Preference Optimization (AMaPO)**. Our approach is designed to directly resolve the Overfitting-Underfitting Dilemma by dynamically adjusting the gradient magnitude for each sample. We build upon the robust SimPO (Meng, Xia, and Chen 2024) framework, but our key innovation lies in replacing its static margin with a principled, instance-wise adaptive margin, $\gamma(x, y_w, y_l)$. The general objective is:

$$\mathcal{L}_{\text{AMaPO}}(\pi_{\theta}; \mathcal{D}) = -\mathbb{E}_{(\mathbf{x}, \mathbf{y}_w, \mathbf{y}_l) \sim \mathcal{D}} \left[\log \sigma \left(r_{\pi_{\theta}}(x, y_w, y_l) - \gamma(x, y_w, y_l) \right) \right], \tag{7}$$

where $r_{\pi_{\theta}}(x,y_w,y_l) = \frac{\beta}{|y_w|} \log \pi_{\theta}(y_w|x) - \frac{\beta}{|y_l|} \log \pi_{\theta}(y_l|x)$ is the implicit ranking accuracy, and $m(x) = \log \sigma(x)$ as Eq. 2. The following subsections detail the design of our adaptive margin, $\gamma(x,y_w,y_l)$.

Formulating the Ideal Adaptive Margin. Our theoretical analysis concluded that an ideal margin must be *dynamically adaptive*. To satisfy this, from definition 2, the margin should reflect the gap between the policy's performance and the ideal target set by the Oracle Ranking Margin, γ^* . We therefore formulate the ideal adaptive margin as:

$$\gamma^*(x, y_w, y_l) = \mathbb{I}[(\gamma^* - r_{\pi_\theta}(x, y_w, y_l)) > 0] \cdot \gamma^*.$$
 (8)

This formulation is inherently dynamic and directly addresses the dilemma. For incorrectly ranked samples where

³For simplicity, we omit the contribution of $\Lambda'(\log \pi_w)$ to the gradient magnitude, as $\Lambda'(\log \pi_w)$ is typically a constant and not related to the γ .

⁴We provide further theoretical analysis in Appendix C.1

⁵The analysis of other methods is in Appendix B.2.

 $r_{\pi_{\theta}} \leq 0 < \gamma^*$, the margin is positive and large, amplifying the corrective gradient to mitigate underfitting. For correctly ranked samples where $r_{\pi_{\theta}} > \gamma^* \geq 0$, the margin becomes zero, suppressing the gradient and preventing overfitting.

Estimating the Oracle Margin in Practice. Since the true Oracle Ranking Margin γ^* is inaccessible, we must estimate it. Motivated by empirical findings that the implicit reward distributions of aligned models are often right-skewed (Qin, Feng, and Yang 2024), we propose using the mean implicit margin μ_r within the current training batch B as a robust, annotation-free proxy for γ^* . To make the ideal margin from Eq. 8 tractable by relaxing the non-negativity constraint (i.e., the $\max(\cdot,0)$ function), while also stabilizing the estimation and scaling it appropriately, we apply Z-score normalization (Patro and Sahu 2015). This yields:

$$\gamma(x, y_w, y_l) = \max\left(\frac{\mu_r - r_{\pi_\theta}(x, y_w, y_l)}{\sigma_r} \cdot \mu_r, 0\right), \quad (9)$$

where μ_r and σ_r are the mean and standard deviation of $r_{\pi_\theta}(x,y_w,y_l)$ computed within batch B. The term $\frac{\mu_r-r_{\pi_\theta}}{\sigma_r}$ calculates the normalized "difficulty" of the sample, which is then scaled by the estimated oracle target μ_r itself.

Margin Scaling for Quality Representation. The margin from Eq. 9 effectively captures the relative difficulty of a sample. However, empirical results find that the log probability value might not truthfully reflect the quality of generated sequence (Holtzman et al. 2021). To better represent the quality gap between responses and speed up the training of the hard incorrectly ranked samples, we introduce a scaling function. Inspired by the strong correlation between perplexity (PPL) and generation quality (Marion et al. 2023; Gonen et al. 2023), we use an exponential scaling function. The scaled margin is ⁶:

$$h_{\gamma}(\gamma) = \begin{cases} 0 & \text{if } \gamma = 0, \\ \beta \cdot e^{\gamma} & \text{if } \gamma > 0. \end{cases}$$
 (10)

Final Objective. Finally, to ensure that our adaptive margin serves as a fixed target for each sample within an optimization step, we apply a stop-gradient operation ($sg[\cdot]$). This prevents the gradient from flowing back through the margin calculation. Incorporating all components, the final AMaPO objective is:

$$\mathcal{L}_{\text{AMaPO}}(\pi_{\theta}; \mathcal{D}) = -\mathbb{E}_{(\mathbf{x}, \mathbf{y}_w, \mathbf{y}_l) \sim \mathcal{D}} \left[\log \sigma \left(r_{\pi_{\theta}}(x, y_w, y_l) - h_{\gamma}(\text{sg}[\gamma(x, y_w, y_l)]) \right) \right]. \tag{11}$$

In summary, by employing an adaptive margin derived from the model's current ranking correctness, AMaPO effectively manipulates the gradient to focus on learning from its errors. This design directly resolves the overfitting and underfitting issues inherent in prior methods, leading to improved ranking accuracy and superior alignment performance.

5 Experiments

This section presents a series of experiments designed to rigorously evaluate AMaPO from multiple perspectives. Our primary goal is to establish its overall superiority against current methods, measured by both ranking accuracy and performance on downstream tasks. Furthermore, we provide a targeted analysis to confirm that AMaPO directly addresses the core overfitting and underfitting issues identified in our framework. Finally, detailed ablation studies to validate the importance of each components.

5.1 Experimental Setup

Basemodels. To assess the robustness and general applicability of our method, we experiment with two widely-used open-source model families: Llama3-8B (AI@Meta 2024) and Mistral-7B (Jiang 2024). For each family, we test two distinct scenarios: (1) a **Base** model setup, where we first perform SFT before preference alignment, and (2) an **Instruct** model setup, where we begin directly with the publicly available instruction-tuned model.

Training Datasets. Our training pipeline for the Base models follows the well-established recipe (Tunstall et al. 2023): we fine-tune on UltraChat-200k (Ding et al. 2023) to create an SFT model, which then is used to for preference optimization on the UltraFeedBack Binarized dataset (Cui et al. 2023). For the Instruct setup, we need to mitigate the distribution shift between the pre-trained instruction model and the preference data (Meng, Xia, and Chen 2024). To ensure a controlled and fair comparison, we regenerate the preference pairs by using the Instruct model itself to generate five candidate responses for each prompt from UltraFeedback. We then use a strong reward model, PairRM (Jiang, Ren, and Lin 2023), to select the best and worst responses, thereby creating a on-distribution preference dataset for the model being trained.

Evaluation benchmarks. Our evaluation is designed to be multi-faceted, assessing performance from ranking accuracy to its practical downstream impact. (1) Ranking Accuracy: To directly validate our claims about improving preference learning, we measure ranking accuracy on RM-Bench (Liu et al. 2024), a challenging benchmark designed to test a model's grasp of subtle preference nuances. (2) Overfitting-underfitting Problem: To further test our hypothesis about resolving this problem, we also evaluate ranking accuracy across four generalization scenarios on UltraFeedBack following (Hong et al. 2025): In-Distribution (ID), Prompt-OOD, Response-OOD, and Mutual-OOD. (3) **Downstream Performance:** To confirm that improved ranking translates to better downstream performance, we evaluate on the popular AlpacaEval 2 (Li et al. 2023) and MT-Bench (Zheng et al. 2023a) benchmarks.

Baselines. We compare AMaPO against a comprehensive suite of strong and recent offline preference optimization methods, including DPO (Rafailov et al. 2023), SLiC (Zhao et al. 2023), IPO (Azar et al. 2024), KTO (Ethayarajh et al. 2024), and SimPO (Meng, Xia, and Chen 2024). To ensure a fair and rigorous comparison, we have thoroughly tuned the

⁶This elegantly transforms our additive, log-space margin into the geometric mean of the PPL ratio within the batch. The derivation is in Appendix C.2.

Table 2: AlpacaEval2 (Li et al. 2023) and MT-Bench (Zheng et al. 2023a) results under the four settings. LC and WR denote
length-controlled and raw win rate, respectively. The best results are highlighted in bold.

	Llama3-8B-Base			Llama3-8B-Instruct			Mistral-7B-Base			Mistral-7B-Instruct		
Method	AlpacaEval 2		MT-Bench	Alpaca	aEval 2	MT-Bench	AlpacaEval 2		MT-Bench	AlpacaEval 2		MT-Bench
	LC (%)	WR (%)	GPT-4 Turbo	LC (%)	WR (%)	GPT-4 Turbo	LC (%)	WR (%)	GPT-4 Turbo	LC (%)	WR (%)	GPT-4 Turbo
SFT	6.2	4.6	3.3	26.0	25.3	6.9	8.4	6.2	4.8	17.1	14.7	6.2
DPO	18.2	15.5	6.5	40.3	37.9	7.0	15.1	12.5	5.9	26.8	24.9	6.3
SLiC	12.3	13.7	6.3	26.9	27.5	6.8	10.9	8.9	5.8	24.1	24.6	6.5
IPO	14.4	14.2	6.5	35.6	35.6	7.0	11.8	9.4	5.5	20.3	20.3	6.4
KTO	14.2	12.4	6.3	33.1	31.8	6.9	13.1	9.1	5.4	24.5	23.6	6.4
CPO	10.8	8.1	6.0	28.9	32.2	7.0	9.8	8.9	5.4	23.8	28.8	6.3
SimPO	22.0	20.3	6.6	44.7	40.5	7.0	21.5	20.8	6.0	32.1	34.8	6.6
$\alpha ext{-DPO}$	21.7	20.6	6.8	46.6	39.6	7.2	17.2	13.0	6.2	34.2	33.8	6.7
AMaPO	26.4	21.4	6.4	46.1	41.3	7.2	24.3	20.6	6.2	34.5	35.1	6.7

Table 3: RM-bench (Liu et al. 2024) results under the three setups, where Easy, Normal and Hard represent the preferred responses have the better, same and worse style compared to less preferred ones. Our AMaPO can achieve good performance on distinguishing responses across various setups.

	Method	Avg.	Easy	Normal	Hard
Mistral-7B Base	DPO SimPO α-DPO AMaPO	55.8 56.5 58.4 58.1	89.8 86.3 86.6 86.4	58.7 58.7 62.7 62.5	18.7 23.5 25.0 25.4
Llama3-8B Base	DPO SimPO α-DPO AMaPO	54.6 56.9 58.2 58.6	91.6 87.5 87.1 87.8	57.4 60.2 62.1 62.6	15.0 23.3 25.6 25.4
Mistral-7B Instruct	DPO SimPO α-DPO AMaPO	53.2 54.9 55.2 55.5	91.3 89.0 90.9 91.4	55.5 57.8 58.4 59.2	12.9 17.8 16.3 15.9
Llama3-8B Instruct	DPO SimPO $\alpha ext{-DPO}$ AMaPO	53.4 55.7 55.0 56.5	89.6 86.1 83.4 85.7	55.4 58.7 57.6 59.8	15.1 22.4 23.8 24.0

hyperparameters for each baseline method and report their best achievable performance. ⁷

5.2 Main Results on Benchmarks

Results on Preference Ranking and Downstream Benchmarks. Our main results demonstrate that AMaPO achieves superior performance in both preference learning and downstream alignment tasks. As shown in Table 3, which evaluates the ability to distinguish subtle preference differences, AMaPO consistently outperforms other methods in different scenarios. Specifically, on the Llama3-8B-Base setup, AMaPO improves the ranking accuracy over the strong SimPO baseline by 2.4 and 2.1 points on Normal and Hard cases, respectively. This highlights its enhanced capability to discern subtle quality variations. In contrast, while DPO often achieves the highest accuracy on Easy cases where style biases can guide the model, it exhibits a

significant performance drop on Normal and Hard ones. For instance, on Mistral-7B-Base model, DPO's accuracy plummets from 89.8% on Easy cases to just 18.7% on Hard ones.

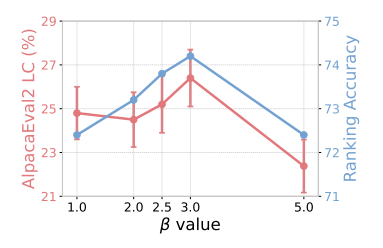
This discrepancy aligns perfectly with our gradient analysis, which identifies DPO's tendency to overfit to simple patterns while underfitting to complex, misranked samples. Although SFT models sometimes perform well, especially on instruct-tuned setups, this strength does not reliably carry over to downstream tasks. In contrast, AMaPO's robust preference learning translates directly into superior alignment. As shown in Table 2, AMaPO consistently leads on AlpacaEval 2 and MT-Bench. Notably, it achieves a length-controlled (LC) win rate up to 4.4 points higher than SimPO on Llama3-8B-Base and demonstrates strong performance gains regardless of the evaluation metric. These findings confirm that AMaPO effectively enhances core ranking capabilities, and this fundamental improvement successfully generalizes to diverse downstream applications. ⁸

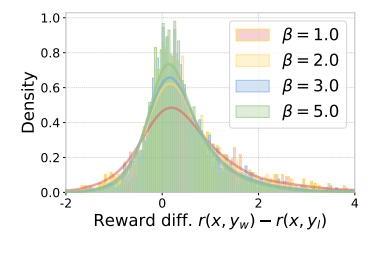
Table 4: Overfitting-underfitting Problem over ultrafeedback dataset following (Lin et al. 2024; Hong et al. 2025). Our AMaPO can achieve promising ranking accuracy across indomain and out-of-distribution settings.

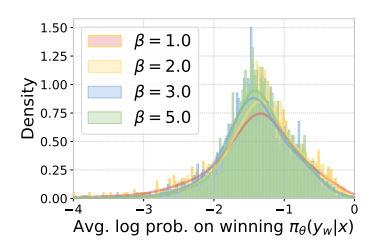
	Method	$\mathcal{D}_{ ext{ID}}$	$\mathcal{D}_{\sim Prompt}$	$\mathcal{D}_{\sim Response}$	$\mathcal{D}_{\sim Mutual}$
Mistral-7B Base	DPO SimPO AMaPO	69.66 78.02 79.26	83.01 91.05 92.46	68.41 76.08 83.62	67.35 75.94 82.97
Llama3-8B Base	DPO SimPO AMaPO	64.73 78.1 77.33	76.2 91.14 91.41	61.29 78.6 77.87	60.25 76.3 76.91
Mistral-7B Instruct	DPO SimPO AMaPO	82.19 81.39 82.85	86.83 95.17 94.88	75.67 86.31 91.74	72.89 85.64 90.91
Llama3-8B Instruct	DPO SimPO AMaPO	79.23 84.45 84.04	87.34 95.68 96.5	67.94 93.46 94.16	66.16 93.16 94.26

⁸For more results like further downstream task results, batch size ablation, generation length, and cases, see Appendices D.3, D.4, D.5, D.6, and E.

⁷Detailed experimental setups are provided in Appendix D.1.







(a) Performance w/ different β

(b) Prob. diff. distribution.

(c) Log prob. distribution.

Figure 1: Ablation studies of the β . (a) Ranking accuracy and AlpacaEval2 LC win rate under different β values. (b) Reward difference distribution under different β values. (c) Log likelihood distribution on chosen responses under different β values.

Results on the Overfitting-Underfitting Problem. To further validate our theoretical claims regarding the overfitting-underfitting dilemma, we evaluate model performance across four generalization scenarios. As shown in Table 4, the results strongly support our analysis and demonstrate the effectiveness of AMaPO. DPO consistently performs the worst across both in-distribution and OOD settings, confirming its dual vulnerability. For example, on the Llama3-8B-Base setup, DPO's accuracy is not only the lowest in-distribution but also fails to generalize, lagging behind AMaPO by over 15 points on Prompt OOD. This aligns with our theory that DPO underfits on challenging OOD samples. SimPO, while achieving high in-distribution accuracy, suggesting a tendency to overfit to seen data, does not generalize as effectively as AMaPO due to its static margin. For instance, on Mistral-7B-Base, SimPO's performance drops by 15 points from Prompt OOD to Mutual OOD. In contrast, AMaPO resolves this tension: it matches or exceeds SimPO's in-distribution performance while achieving the best results across all OOD settings. This robust generalization confirms that our adaptive margin successfully mitigates the overfitting-underfitting problem we identified.

Table 5: Ablation studies under Llama3-8B setups. We ablate the key design of AMaPO and explore variants of the adaptive margin.

	Lla	ama3-8	B-Base	Llama3-8B-Instruct			
Method	AlpacaEval 2		MT-Bench	Alpac	aEval 2	MT-Bench	
	LC (%)	WR (%)	GPT-4 Turbo	LC (%)	WR (%)	GPT-4 Turbo	
DPO SimPO	18.2 22.0	15.5 20.3	6.5 6.6	40.3 44.7	37.9 40.5	7.0 7.0	
AMaPO	26.3	21.4	6.5	46.1	41.3	7.2	
w/o Z-norm w/o exp w/o adaptive w/o zero	24.8 24.0 20.7 22.3	20.4 17.6 16.4 21.1	6.3 6.1 6.3 6.6	44.2 47.1 47.2 48.6	39.6 42.9 42.5 45.0	7.0 7.0 7.0 6.7	

5.3 Ablations and Further Analysis

This section delves deeper into the components and behavior of AMaPO. We begin by ablating the modules, such as Z-normalization and exponential scaling, to confirm their necessity. Our main analysis then focuses on the hyperparameter β , which controls the strength of the adaptive margin.

Importance of the components of AMaPO. Due to the significant computational resources required, we conduct this ablation study on the Llama3-8B-Base and Llama3-8B-Instruct models, evaluating performance on key downstream benchmarks. Our results in Table 5 shows that the complete AMaPO design, which integrates Z-normalization (can also been shown as an alternative of linear scaling functions), exponential scaling, and a zero margin for correctly ranked samples, is critical for achieving robust and well-rounded performance. While most ablated variants still outperform the DPO baseline, removing any single component results in a notable performance degradation. This is particularly evident on the Llama3-8B-Base model, where removing exponential scaling and Z-normalization ('w/o adaptive') degrades the AlpacaEval 2 LC and WR to 20.7% and 16.7%, below the full AMaPO's 26.3% and 21.4%. Similarly, removing any components of AMaPO on the Llama3-8B-Instruct model causes the score on MT-Bench to drop from AMaPO's 7.2 to about 7.0. Thus, the synergistic combination of all components in AMaPO is essential for a better adaptive margin and ensuring consistently superior performance across diverse evaluation settings.

Influence of β . To investigate the influence of our sole hyperparameter, β , we trained AMaPO on the UltraFeedback dataset using the Llama 3-8B-Base model with varying β values. As shown in Figure 1a, our analysis on the AlpacaEval 2 and UltraFeedback test sets reveals a clear inverted Ushaped relationship between β and performance. Both ranking accuracy and the LC win rate initially increase with β before declining, indicating that an optimal regularization strength is empirically around $\beta = 3$. The underlying reason for this trend is revealed by analyzing the probability distributions on the UltraFeedback test set (Figures 1b and 1c). As β increases, the distribution of the probability margin, $\pi_{\theta}(y_w|x) - \pi_{\theta}(y_l|x)$, sharpens significantly, but the value at the peak of the likelihood of winning responses, $\pi_{\theta}(y_w|x)$, decreases. This reveals a critical trade-off: while a stronger regularization (a higher β) initially forces the model to more accurately fit our adaptive margin, leading to performance gains, an excessively high β causes the likelihood distribution to become overly peaked, resulting in model degeneration and a subsequent drop in performance.

6 Conclusion

In this work, we presented a novel analysis of offline preference optimization and proposed a new algorithm, AMaPO, to address the dilemma we identified. Through a unified margin-based framework, our gradient analysis revealed that methods like DPO suffer from an overfitting-underfitting dilemma, inefficiently learning from preference data. AMaPO rectifies this by introducing an instance-wise adaptive margin that intelligently prioritizes difficult, misranked samples while ignoring those already learned. Extensive experiments show that AMaPO has a better ranking accuracy, leading to a better performance on downstream tasks. By providing both a more effective alignment algorithm and a sharper analytical lens, this work paves the way for more principled advances in preference optimization. ⁹

Acknowledgments

This work was supported in part by the National Natural Science Foundation of China (No. 62272330, and No. U24A20328), and in part by the Science Fund for Creative Research Groups of Sichuan Province Natural Science Foundation (No. 2024NSFTD0035).

References

AI@Meta. 2024. Llama 3 Model Card.

Amini, A.; Vieira, T.; and Cotterell, R. 2024. Direct Preference Optimization with an Offset. In *ACL (Findings)*.

Azar, M. G.; Guo, Z. D.; Piot, B.; Munos, R.; Rowland, M.; Valko, M.; and Calandriello, D. 2024. A general theoretical paradigm to understand learning from human preferences. In *International Conference on Artificial Intelligence and Statistics*, 4447–4455. PMLR.

Bai, Y.; Jones, A.; Ndousse, K.; Askell, A.; Chen, A.; Das-Sarma, N.; Drain, D.; Fort, S.; Ganguli, D.; Henighan, T.; et al. 2022. Training a helpful and harmless assistant with reinforcement learning from human feedback. *arXiv preprint arXiv:2204.05862*.

Boser, B. E.; Guyon, I. M.; and Vapnik, V. N. 1992. A training algorithm for optimal margin classifiers. In *Proceedings of the fifth annual workshop on Computational learning theory*, 144–152.

Bradley, R. A.; and Terry, M. E. 1952. Rank analysis of incomplete block designs: I. The method of paired comparisons. *Biometrika*, 39(3/4): 324–345.

Chen, A.; Malladi, S.; Zhang, L.; Chen, X.; Zhang, Q. R.; Ranganath, R.; and Cho, K. 2024. Preference learning algorithms do not learn preference rankings. *Advances in Neural Information Processing Systems*, 37: 101928–101968.

Clark, P.; Cowhey, I.; Etzioni, O.; Khot, T.; Sabharwal, A.; Schoenick, C.; and Tafjord, O. 2018. Think you have solved question answering? try arc, the ai2 reasoning challenge. *arXiv* preprint arXiv:1803.05457.

Cui, G.; Yuan, L.; Ding, N.; Yao, G.; Zhu, W.; Ni, Y.; Xie, G.; Liu, Z.; and Sun, M. 2023. Ultrafeedback: Boosting language models with high-quality feedback.

Ding, N.; Chen, Y.; Xu, B.; Qin, Y.; Hu, S.; Liu, Z.; Sun, M.; and Zhou, B. 2023. Enhancing Chat Language Models by Scaling High-quality Instructional Conversations. In *Proceedings of the 2023 Conference on Empirical Methods in Natural Language Processing*, 3029–3051.

Engstrom, L.; Ilyas, A.; Santurkar, S.; Tsipras, D.; Janoos, F.; Rudolph, L.; and Madry, A. 2020. Implementation matters in deep policy gradients: A case study on ppo and trpo. *arXiv preprint arXiv:2005.12729*.

Ethayarajh, K.; Xu, W.; Muennighoff, N.; Jurafsky, D.; and Kiela, D. 2024. KTO: Model Alignment as Prospect Theoretic Optimization. arXiv:2402.01306.

Feng, D.; Qin, B.; Huang, C.; Zhang, Z.; and Lei, W. 2024. Towards analyzing and understanding the limitations of dpo: A theoretical perspective. *arXiv preprint arXiv:2404.04626*. Gao, L.; Tow, J.; Abbasi, B.; Biderman, S.; Black, S.; DiPofi, A.; Foster, C.; Golding, L.; Hsu, J.; Le Noac'h, A.; Li, H.; McDonell, K.; Muennighoff, N.; Ociepa, C.; Phang, J.; Reynolds, L.; Schoelkopf, H.; Skowron, A.; Sutawika, L.; Tang, E.; Thite, A.; Wang, B.; Wang, K.; and Zou, A. 2024. The Language Model Evaluation Harness.

Gonen, H.; Iyer, S.; Blevins, T.; Smith, N. A.; and Zettlemoyer, L. 2023. Demystifying Prompts in Language Models via Perplexity Estimation. In *Findings of the Association for Computational Linguistics: EMNLP 2023*, 10136–10148.

Gorbatovski, A.; Shaposhnikov, B.; Malakhov, A.; Surnachev, N.; Aksenov, Y.; Maksimov, I.; Balagansky, N.; and Gavrilov, D. 2024. Learn your reference model for real good alignment. *arXiv preprint arXiv:2404.09656*.

Hendrycks, D.; Burns, C.; Kadavath, S.; Arora, A.; Basart, S.; Tang, E.; Song, D.; and Steinhardt, J. 2021. Measuring mathematical problem solving with the math dataset. *arXiv* preprint arXiv:2103.03874.

Holtzman, A.; West, P.; Shwartz, V.; Choi, Y.; and Zettlemoyer, L. 2021. Surface Form Competition: Why the Highest Probability Answer Isn't Always Right. In *Proceedings of the 2021 Conference on Empirical Methods in Natural Language Processing*, 7038–7051.

Hong, J.; Lee, N.; Kim, E.; Son, G.; Chung, W.; Gupta, A.; Tang, S.; and Thorne, J. 2025. On the Robustness of Reward Models for Language Model Alignment. *arXiv preprint arXiv:2505.07271*.

Jiang, D.; Ren, X.; and Lin, B. Y. 2023. LLM-Blender: Ensembling Large Language Models with Pairwise Ranking and Generative Fusion. In *Proceedings of the 61st Annual Meeting of the Association for Computational Linguistics (Volume 1: Long Papers)*, 14165–14178.

Jiang, F. 2024. *Identifying and mitigating vulnerabilities in llm-integrated applications*. Master's thesis, University of Washington.

Kim, K.; Seo, A.; Liu, H.; Shin, J.; and Lee, K. 2024. Margin Matching Preference Optimization: Enhanced Model Alignment with Granular Feedback. In *Findings of the Association for Computational Linguistics: EMNLP 2024*, 13554–13570.

Kingma, D. P. 2014. Adam: A method for stochastic optimization. *arXiv preprint arXiv:1412.6980*.

 $^{^9\}mathrm{A}$ detailed discussion of limitations can be found in Appendix A.

- Li, X.; Zhang, T.; Dubois, Y.; Taori, R.; Gulrajani, I.; Guestrin, C.; Liang, P.; and Hashimoto, T. B. 2023. AlpacaEval: An Automatic Evaluator of Instruction-following Models. https://github.com/tatsu-lab/alpaca_eval.
- Lin, S.; Hilton, J.; and Evans, O. 2021. Truthfulqa: Measuring how models mimic human falsehoods. *arXiv preprint arXiv:2109.07958*.
- Lin, Y.; Seto, S.; Ter Hoeve, M.; Metcalf, K.; Theobald, B.-J.; Wang, X.; Zhang, Y.; Huang, C.; and Zhang, T. 2024. On the limited generalization capability of the implicit reward model induced by direct preference optimization. *arXiv* preprint arXiv:2409.03650.
- Liu, T.; Yu, X.; Zhou, W.; Gu, J.; and Tresp, V. 2025. FocalPO: Enhancing Preference Optimizing by Focusing on Correct Preference Rankings. *arXiv* preprint *arXiv*:2501.06645.
- Liu, T.; Zhao, Y.; Joshi, R.; Khalman, M.; Saleh, M.; Liu, P. J.; and Liu, J. 2023. Statistical rejection sampling improves preference optimization. *arXiv preprint arXiv:2309.06657*.
- Liu, Y.; Liu, P.; and Cohan, A. 2024. Understanding reference policies in direct preference optimization. *arXiv* preprint arXiv:2407.13709.
- Liu, Y.; Yao, Z.; Min, R.; Cao, Y.; Hou, L.; and Li, J. 2024. RM-bench: Benchmarking reward models of language models with subtlety and style. *arXiv preprint arXiv:2410.16184*.
- Ma, Q.; Shi, J.; Jin, C.; Hwang, J.-N.; Belongie, S.; and Li, L. 2025. Gradient Imbalance in Direct Preference Optimization. *arXiv preprint arXiv:2502.20847*.
- Marion, M.; Üstün, A.; Pozzobon, L.; Wang, A.; Fadaee, M.; and Hooker, S. 2023. When less is more: Investigating data pruning for pretraining llms at scale. *arXiv preprint arXiv:2309.04564*.
- Meng, Y.; Xia, M.; and Chen, D. 2024. Simpo: Simple preference optimization with a reference-free reward. *Advances in Neural Information Processing Systems*, 37: 124198–124235.
- Ouyang, L.; Wu, J.; Jiang, X.; Almeida, D.; Wainwright, C.; Mishkin, P.; Zhang, C.; Agarwal, S.; Slama, K.; Ray, A.; et al. 2022. Training language models to follow instructions with human feedback. *Advances in neural information processing systems*, 35: 27730–27744.
- Patro, S.; and Sahu, K. K. 2015. Normalization: A preprocessing stage. *arXiv preprint arXiv:1503.06462*.
- Qin, B.; Feng, D.; and Yang, X. 2024. Towards understanding the influence of reward margin on preference model performance. *arXiv* preprint arXiv:2404.04932.
- Rafailov, R.; Sharma, A.; Mitchell, E.; Manning, C. D.; Ermon, S.; and Finn, C. 2023. Direct preference optimization: Your language model is secretly a reward model. *Advances in Neural Information Processing Systems*, 36: 53728–53741.
- Rein, D.; Hou, B. L.; Stickland, A. C.; Petty, J.; Pang, R. Y.; Dirani, J.; Michael, J.; and Bowman, S. R. 2024. Gpqa: A graduate-level google-proof q&a benchmark. In *First Conference on Language Modeling*.

- Sakaguchi, K.; Bras, R. L.; Bhagavatula, C.; and Choi, Y. 2021. Winogrande: An adversarial winograd schema challenge at scale. *Communications of the ACM*, 64(9): 99–106. Schulman, J.; Wolski, F.; Dhariwal, P.; Radford, A.; and Klimov, O. 2017. Proximal Policy Optimization Algorithms. arXiv:1707.06347.
- Suzgun, M.; Scales, N.; Schärli, N.; Gehrmann, S.; Tay, Y.; Chung, H. W.; Chowdhery, A.; Le, Q. V.; Chi, E. H.; Zhou, D.; et al. 2022. Challenging big-bench tasks and whether chain-of-thought can solve them. *arXiv preprint arXiv:2210.09261*.
- Tajwar, F.; Singh, A.; Sharma, A.; Rafailov, R.; Schneider, J.; Xie, T.; Ermon, S.; Finn, C.; and Kumar, A. 2024. Preference Fine-Tuning of LLMs Should Leverage Suboptimal, On-Policy Data. In *International Conference on Machine Learning*, 47441–47474. PMLR.
- Tunstall, L.; Beeching, E.; Lambert, N.; Rajani, N.; Rasul, K.; Belkada, Y.; Huang, S.; Von Werra, L.; Fourrier, C.; Habib, N.; et al. 2023. Zephyr: Direct distillation of Im alignment. *arXiv preprint arXiv:2310.16944*.
- Turner, H.; and Firth, D. 2012. Bradley-Terry models in R: the BradleyTerry2 package. *Journal of Statistical Software*, 48: 1–21.
- Wang, Y.; Ma, X.; Zhang, G.; Ni, Y.; Chandra, A.; Guo, S.; Ren, W.; Arulraj, A.; He, X.; Jiang, Z.; et al. 2024. Mmlu-pro: A more robust and challenging multi-task language understanding benchmark. In *The Thirty-eight Conference on Neural Information Processing Systems Datasets and Benchmarks Track*.
- Wu, J.; Wang, X.; Yang, Z.; Wu, J.; Gao, J.; Ding, B.; Wang, X.; and He, X. 2024. $\ \alpha$ -DPO: Adaptive Reward Margin is What Direct Preference Optimization Needs. *arXiv preprint arXiv:2410.10148*.
- Xiao, T.; Yuan, Y.; Chen, Z.; Li, M.; Liang, S.; Ren, Z.; and Honavar, V. G. 2025. SimPER: A Minimalist Approach to Preference Alignment without Hyperparameters. *arXiv* preprint arXiv:2502.00883.
- Xiao, T.; Yuan, Y.; Zhu, H.; Li, M.; and Honavar, V. G. 2024. Cal-dpo: Calibrated direct preference optimization for language model alignment. *arXiv preprint arXiv:2412.14516*.
- Xu, H.; Sharaf, A.; Chen, Y.; Tan, W.; Shen, L.; Van Durme, B.; Murray, K.; and Kim, Y. J. 2024. Contrastive Preference Optimization: Pushing the Boundaries of LLM Performance in Machine Translation. In *International Conference on Machine Learning*, 55204–55224. PMLR.
- Yan, Y.; Miao, Y.; Li, J.; Zhang, Y.; Xie, J.; Deng, Z.; and Yan, D. 2024. 3d-properties: Identifying challenges in dpo and charting a path forward. *arXiv preprint arXiv:2406.07327*.
- Yuan, H.; Zeng, Y.; Wu, Y.; Wang, H.; Wang, M.; and Leqi, L. 2024. A Common Pitfall of Margin-based Language Model Alignment: Gradient Entanglement. *arXiv preprint arXiv:2410.13828*.
- Zhao, H.; Winata, G. I.; Das, A.; Zhang, S.-X.; Yao, D. D.; Tang, W.; and Sahu, S. 2024. Rainbowpo: A unified framework for combining improvements in preference optimization. *arXiv* preprint arXiv:2410.04203.

Zhao, Y.; Joshi, R.; Liu, T.; Khalman, M.; Saleh, M.; and Liu, P. J. 2023. Slic-hf: Sequence likelihood calibration with human feedback. *arXiv preprint arXiv:2305.10425*.

Zheng, L.; Chiang, W.-L.; Sheng, Y.; Zhuang, S.; Wu, Z.; Zhuang, Y.; Lin, Z.; Li, Z.; Li, D.; Xing, E.; et al. 2023a. Judging llm-as-a-judge with mt-bench and chatbot arena. *Advances in Neural Information Processing Systems*, 36: 46595–46623.

Zheng, R.; Dou, S.; Gao, S.; Hua, Y.; Shen, W.; Wang, B.; Liu, Y.; Jin, S.; Liu, Q.; Zhou, Y.; et al. 2023b. Secrets of rlhf in large language models part i: Ppo. *arXiv preprint arXiv:2307.04964*.

Zhou, J.; Lu, T.; Mishra, S.; Brahma, S.; Basu, S.; Luan, Y.; Zhou, D.; and Hou, L. 2023. Instruction-following evaluation for large language models. *arXiv preprint arXiv:2311.07911*.

A Limitations and Future Work

While our work introduces a principled approach to preference optimization and demonstrates its effectiveness, we identify several promising avenues for future research that arise from the scope and limitations of our study.

Scaling. Our experiments were conducted on models up to the 8B parameter scale. A crucial next step is to investigate the performance and dynamics of AMaPO on much larger models (e.g., 70B and beyond), where phenomena like overfitting and underfitting may manifest differently.

Generality of the Oracle Margin Estimator. We propose using the batch-wise mean implicit margin as a practical and effective proxy for the inaccessible Oracle Ranking Margin. However, the optimality of this non-parametric estimator may not be universal. Its performance could be influenced by factors such as the quality and diversity of the initial SFT model or the noise level and distribution of the preference dataset. Future research could explore more sophisticated estimators for the oracle margin, potentially involving lightweight parametric models or meta-learning approaches, to further enhance the adaptability of the margin.

Alternatives of scaling functions. In this work, the scaling function serves to appropriately amplify the gradient magnitude of hard, incorrectly ranked samples. AMaPO exclusively consider the widely-used exponential function and Z-normalization as the nonlinear and linear scaling functions, respectively, which elegantly transform our additive, log-space margin into the geometric mean of the PPL ratio within the batch. Although our ablation studies demonstrate that the popular linear and non-linear function do work, a comprehensive exploration of better scaling functions would further improve the margin-based preference optimization algorithms.

Scope of the Gradient Analysis. Our theoretical motivation is grounded in a gradient-level analysis that examines the instantaneous effect of the margin on the learning signal. This static snapshot is powerful for algorithm design but does not constitute a full analysis of the dynamic training process over time. A compelling direction for future work would be to study the entire training trajectory, exploring how AMaPO's adaptive margin influences the loss landscape, convergence properties, and the evolution of the model's internal representations throughout the optimization process.

B Gradient Analysis

In this section, we employ the unified framework to analyze other methods in detail.

B.1 Baseline Methods

We also provides a detailed introduction to other state-ofthe-art baselines of offline preference optimization, with an emphasis on the design of the margin in their learning objectives.

IPO Identity Preference Optimization (Azar et al. 2024) minimizes a squared loss regression problem by defining an

alternative reward function, avoiding unstable RL training. IPO involves one hyperparameter, β , to adjust the reward margin.

$$\mathcal{L}_{\text{IPO}} = -\left[\left(\log \frac{\pi_{\theta}(y_w|x)}{\pi_{\theta}(y_t|x)} - \log \frac{\pi_{\text{ref}}(y_w|x)}{\pi_{\text{ref}}(y_t|x)} - \frac{1}{2\beta} \right)^2 \right].$$

SLiC Sequence Likelihood Calibration (Zhao et al. 2023) directly uses log-likelihood as a ranking loss and includes a SFT objective to prevent degeneration. SLiC designs a hyperparameter δ as the margin for the ranking loss, where the ranking loss decreases with the ranking margin increases.

$$\mathcal{L}_{\text{SLiC}} = \max\left(0, \delta - \log \frac{\pi_{\theta}(y_w \mid x)}{\pi_{\theta}(y_l \mid x)}\right) - \lambda \log \pi_{\theta}(y_w \mid x).$$

It can also be interpreted as an hinge loss variation of DPO (Liu et al. 2023) as follows:

$$\mathcal{L}_{\text{SLiC}} = \max \left\{ 0, 1 - \tau \left(\log \frac{\pi_{\theta}(y_w|x)}{\pi_{\theta}(y_l|x)} - \log \frac{\pi_{\text{ref}}(y_w|x)}{\pi_{\text{ref}}(y_l|x)} \right) \right\},\,$$

where $\tau = \frac{1}{\delta}$ denotes the true label in hinge loss.

CPO Contrastive Preference Optimization (Xu et al. 2024) uses log-likelihood as the reward and introduces an explicit regularization with Supervised Fine-Tuning (SFT) objective rather than the reward margin in BT-model, while eliminating the need for the reference policy.

$$\mathcal{L}_{\text{CPO}} = -\log \sigma \left(\beta \log \frac{\pi_{\theta}(y_w \mid x)}{\pi_{\theta}(y_l \mid x)}\right) - \lambda \log \pi_{\theta}(y_w \mid x).$$

ODPO Direct Preference Optimization with an offset (Amini, Vieira, and Cotterell 2024) incorporates additional ground-truth reward values from external reward model and employs the reward values difference Δ_r as an instance-wise margin.

$$\mathcal{L}_{\text{ODPO}} = -\left[\log \sigma \left(\beta \log \frac{\pi_{\theta}(y_w|x)}{\pi_{\theta}(y_t|x)} - \beta \log \frac{\pi_{\text{ref}}(y_w|x)}{\pi_{\text{ref}}(y_t|x)}\right) - \Delta_r\right].$$

FocalPO FocalPO (Liu et al. 2025) downweighs misranked preference pairs and prioritizes enhancing the model's understanding of pairs that it can already rank correctly.

$$\mathcal{L}_{\text{FocalPO}} = -\left[p^{\gamma}\left(y_{w} \succ y_{l} \mid x\right) \log p\left(y_{w} \succ y_{l} \mid x\right)\right].$$

where $p\left(y_w \succ y_l | x\right) = \sigma(\beta \log \frac{\pi_{\theta}(y_w | x)}{\pi_{\theta}(y_l | x)} - \beta \log \frac{\pi_{\text{ref}}(y_w | x)}{\pi_{\text{ref}}(y_l | x)})$.

KTO Kahneman-Tversky Optimization (Ethayarajh et al. 2024) learns from non-paired preference data to adapt to a board usage.

$$\mathcal{L}_{\text{KTO}} = -\lambda_w \sigma \left(\beta \log \frac{\pi_{\theta}(y_w|x)}{\pi_{\text{ref}}(y_w|x)} - z_{\text{ref}} \right) + \lambda_l \sigma \left(z_{\text{ref}} - \beta \log \frac{\pi_{\theta}(y_t|x)}{\pi_{\text{ref}}(y_t|x)} \right),$$

where $z_{\text{ref}} = \mathbb{E}_{(x,y) \sim \mathcal{D}} \left[\beta \text{KL}(\pi_{\theta}(y \mid x) || \pi_{\text{ref}}(y \mid x)) \right].$

 α -**DPO** Adaptive Reward Margin for Direct Preference Optimization (Wu et al. 2024) interpolates between policy-driven specialization and uniform exploration while enabling instance-adaptive reward margins.

$$\mathcal{L}_{\alpha-\text{DPO}} = -\left[\log \sigma \left(u(x, y_w, y_l) - \text{sg}\left[\gamma + \alpha M^*(x, y_w, y_l)\right]\right)\right].$$

where $u(x,y_w,y_l)=\frac{\beta}{|y_w|}\log\pi_\theta(y_w|x)-\frac{\beta}{|y_l|}\log\pi_\theta(y_l|x),$ $M(x,y_w,y_l)=\beta\log\frac{\pi_\theta(y_w|x)\pi_{\rm ref}(y_l|x)}{\pi_{\rm ref}(y_w|x)\pi_\theta(y_l|x)},$ M^* represents applying Z-normalization to M across training dataset, γ is a tunable constant margin and sg represent stop gradient.

Under our unified margin framework Eq. 2, they are shown as Table 6.

B.2 Gradient Analysis

We further analyze the gradients of the aforementioned objectives under our unified framework Eq. 5 (except DPO and SimPO) to understand the influence of the margin. For notational simplicity, we sometimes omit the β in the following derivations, and $\pi_{\theta}(x, y_w, y_l) = \log \pi_{\theta}(y_w|x) - \log \pi_{\theta}(y_l|x)$.

IPO The gradient magnitude d_{θ} is a monotonically increasing function.

$$\nabla_{\boldsymbol{\theta}} \mathcal{L}_{\text{IPO}} (\boldsymbol{\theta}) = -\underbrace{2(\pi_{\boldsymbol{\theta}}(x, y_w, y_l) - (c_{\text{ref}} + \frac{1}{2\beta}))}_{\text{gradient magnitude } d_{\boldsymbol{\theta}}}$$
$$(\nabla \log \pi_w - \nabla \log \pi_l).$$

The margin, $\gamma=c_{\rm ref}+\frac{1}{2\beta}$, derived from the reference model and calibrated reward margin, might result in overfitting and underfitting, similar to DPO.

SLiC Considering $1-\tau(\log\frac{\pi_{\theta}(y_w|x)}{\pi_{\theta}(y_l|x)}-\log\frac{\pi_{\mathrm{ref}}(y_w|x)}{\pi_{\mathrm{ref}}(y_l|x)})>0$, i.e., when the gradient exists. The gradient magnitude d_{θ} is a monotonically increasing function. The margin, $\gamma=c_{\mathrm{ref}}$, derived from the reference model, might also result in underfitting.

$$\nabla_{\theta} \mathcal{L}_{\mathrm{SLiC}} (\theta) = -\underbrace{\tau(\pi_{\theta}(x, y_w, y_l) - c_{\mathrm{ref}})}_{\text{gradient magnitude } d_{\theta}}$$
$$(\nabla \log \pi_w - \nabla \log \pi_l).$$

CPO The first gradient magnitude $d_{\pmb{\theta}}^w$ is monotonically increasing, where the explicit regularization with SFT $\lambda>0$ manipulates the gradient magnitude. However, the margin, $\gamma=0$, might result in underfitting. And $d_{\pmb{\theta}}^l$ likewise.

$$\nabla_{\boldsymbol{\theta}} \mathcal{L}_{\text{CPO}} \left(\boldsymbol{\theta} \right) = \underbrace{\left(\sigma \left(\pi_{\boldsymbol{\theta}}(\boldsymbol{x}, y_w, y_l) \right) - 1 - \lambda \right)}_{\text{gradient magnitude } d_{\boldsymbol{\theta}}^w} \nabla \log \pi_w \\ + \underbrace{\left(1 - \sigma \left(\pi_{\boldsymbol{\theta}}(\boldsymbol{x}, y_w, y_l) \right) \right)}_{\text{gradient magnitude } d_{\boldsymbol{\theta}}^l} \nabla \log \pi_l,$$

where
$$\pi_{\theta}(x, y_w, y_l) = \log \pi_{\theta}(y_w|x) - \log \pi_{\theta}(y_l|x)$$
.

Table 6: The state-of-the-art baselines for offline preference optimization objectives under our unified framework. Constants satisfy $\beta, \gamma, \delta, \Delta_r, \lambda_w, \lambda_l > 0$, and where $c_{\rm ref}^w = \log \pi_{\rm ref}(y_l|x)$, $c_{\rm ref}^l = \log \pi_{\rm ref}(y_l|x)$, $c_{\rm ref}^l = c_{\rm ref}^w - c_{\rm ref}^l$

	m(a)	$h_w(a)$	$h_l(a)$	γ	$\Lambda(a)$
DPO (Rafailov et al. 2023)	$\log \sigma(a)$	βa	eta a	βc_{ref}	-
IPO (Azar et al. 2024)	a^2	a	a	$c_{\text{ref}} + \frac{1}{2\beta}$	-
SLiC (Zhao et al. 2023)	$\max(0, 1 - \tau \cdot a)$	a	a	$c_{ m ref}$	-
CPO (Xu et al. 2024)	$\log \sigma(a)$	eta a	eta a	-	λa
ODPO (Amini, Vieira, and Cotterell 2024)	$\log \sigma(a)$	eta a	eta a	$\beta c_{\rm ref} + \Delta_r$	-
KTO (Ethayarajh et al. 2024)	a	$\lambda_w \sigma (\beta a - \beta c_{\rm ref}^w - z_{\rm ref})$	$\lambda_l \sigma(\beta c_{\rm ref}^l - \beta a + z_{\rm ref})$	-	-
SimPO (Meng, Xia, and Chen 2024)	$\log \sigma(a)$	$\frac{\beta}{ y_w }a$	$\frac{\beta}{ y_l }a$	γ	-
FocalPO (Liu et al. 2025)	$\sigma^{\gamma}(a)\log\sigma(a)$	$\overset{\circ gw}{eta a}$	$\overset{\circ}{eta}\overset{\circ}{a}$	$eta c_{ ext{ref}}$	-
α -DPO (Wu et al. 2024)	$\log \sigma(a)$	$rac{eta}{ y_w }a$	$rac{eta}{ y_l }a$	$\gamma + \alpha M^*$	-

ODPO The gradient magnitude d_{θ} is a monotonically decreasing function. The margin, $\gamma = c_{\rm ref} + \Delta_r$ derived from the reference model and annotated reward margin, might result in overfitting and underfitting, similar to DPO.

$$\nabla_{\theta} \mathcal{L}_{\text{ODPO}}(\theta) = -\underbrace{\left(1 - \sigma(\pi_{\theta}(x, y_w, y_l) - (c_{\text{ref}} + \Delta_r)\right)}_{\text{gradient magnitude } d_{\theta}}$$

$$(\nabla \log \pi_w - \nabla \log \pi_l).$$

FocalPO The gradient magnitude d_{θ} is monotonically decreasing for $\sigma(u) < e^{-\frac{1}{\gamma}}$, and monotonically increasing for $\sigma(u) > e^{-\frac{1}{\gamma}}$. When applied to the uncommon case of a nonmonotonic d_{θ} , our theoretical framework does not readily yield a definitive conclusion, necessitating further analysis.

$$\begin{split} \nabla_{\theta} \mathcal{L}_{\text{FocalPO}} \left(\theta \right) = & \underbrace{ \sigma(u)^{\gamma} (1 - \sigma(u)) (\gamma \log \sigma(u) + 1) }_{\text{gradient magnitude } d_{\theta}} \\ & (\nabla \log \pi_w - \nabla \log \pi_l). \end{split}$$

where $u = \pi_{\theta}(x, y_w, y_l) - c_{ref}$

KTO The gradient magnitude $d_{\pmb{\theta}}^w$ is monotonically increasing when $\beta \log \pi_{\pmb{\theta}}(y_w|x) - (\beta c_{\mathrm{ref}}^w + z_{\mathrm{ref}}) < 0$, and monotonically decreasing when $\beta \log \pi_{\pmb{\theta}}(y_w|x) - (\beta c_{\mathrm{ref}}^w + z_{\mathrm{ref}}) > 0$. Therefore, we can view $\beta c_{\mathrm{ref}}^w + z_{\mathrm{ref}}$ as the margin of KTO, which is derived from the reference model and KL divergence. However, the margin might result in overfitting and underfitting, similar to DPO. And $d_{\pmb{\theta}}^l$ likewise.

$$\begin{split} \nabla_{\theta} \mathcal{L}_{\mathrm{KTO}} \left(\theta \right) &= - \underbrace{\lambda_w \sigma_w (1 - \sigma_w)}_{\text{gradient magnitude } d_{\theta}^w} \nabla \log \pi_w \\ &+ \underbrace{\lambda_l \sigma_l (1 - \sigma_l)}_{\text{gradient magnitude } d_{\theta}^l} \nabla \log \pi_l, \end{split}$$

where $\sigma_w = \sigma(\beta \log \pi_{\theta}(y_w|x) - (\beta c_{\text{ref}}^w + z_{\text{ref}}))$ and $\sigma_l = \sigma(\beta c_{\text{ref}}^l + z_{\text{ref}} - \beta \log \pi_{\theta}(y_l|x))$.

 α -DPO The gradient magnitude d_{θ} is a monotonically decreasing function. The margin, $\gamma + \alpha M^*$ derived from policy-driven specialization and a tunable target margin, might result in overfitting and underfitting, similar to DPO,

while introducing multiple tunable hyperparameters.

$$\nabla_{\theta} \mathcal{L}_{\alpha-\text{DPO}}(\theta) = -\underbrace{\left(1 - \sigma(\pi_{\theta}(x, y_w, y_l) - (\gamma + \alpha M^*)\right)}_{\text{gradient magnitude} d_{\theta}}$$
$$(\nabla \log \pi_w - \nabla \log \pi_l).$$

C Further Theoretical Analysis

C.1 Analysis towards Oracle Ranking Margin

We have empirically claimed that Oracle Ranking Margin γ^* is an instance-specific, non-negative threshold, as stated in our Definition 2:

$$\gamma^* = r^*(x, y_w) - r^*(x, y_l)$$

where $r^*(\cdot)$ represents the optimal reward function.

Here, we theoretically verify our claim regarding the properties of γ^* based on the theoretical analysis and proof in (Rafailov et al. 2023; Liu, Liu, and Cohan 2024):

Lemma 1 All reward classes under the BT model can be represented with the reparameterization $r(x,y) = \beta \log \pi_{\theta}(y|x)$ for some policy model $\pi_{\theta}(y|x)$.

Therefore, the optimal reward function $r^*(\cdot)$ can be reparameterized with a certain policy model $\pi_{\theta}^*(y|x)$ as follows:

$$\gamma^*(x, y_w, y_l) = \beta \log \pi_\theta^*(x|y_w) - \beta \log \pi_\theta^*(x|y_l)$$
 (12)

where $\pi_{\theta}^*(x|y)$ varies with x and y, and thus γ^* should be an instance-specific threshold $\gamma^*(x,y_w,y_l)$.

Meanwhile, the reparameterization of γ^* as presented in Eq 12 lends theoretical backing to our estimation method for γ^* in Eq 9, which leverages the mean log probability of responses within the current training batch to estimate γ^* .

C.2 Derivations for Margin Scaling

In our method, we introduced the exponential scaling function, $h_{\gamma}(\gamma)$, with the motivation that it better represents the quality gap between responses by leveraging perplexity (PPL). This appendix provides the formal mathematical justification for this choice. We will show that the exponential form has a compelling and intuitive interpretation: it is directly related to the geometric mean of the PPL ratios between the losing and winning responses, adjusted by the sample's specific difficulty.

For $\gamma > 0$ in Eq. 10, we have

$$h_{\gamma}(\gamma) = \beta e^{\gamma} = \beta e^{\alpha \mu_r} = \beta (e^{\mu_r})^{\alpha}$$

where $\alpha=\frac{\mu_r-r_{\pi_\theta}(x,y_w,y_l)}{\sigma_r}$ is the Z-normalization coefficient for $r_{\pi_\theta}(x,y_w,y_l)$, and β is the scaling constant. Therefore, we can focus on e^{μ_r} , where

$$\begin{split} e^{\mu_{\gamma}} = & \exp(\frac{1}{|B|} \sum_{i=1}^{|B|} |y_{w}^{i}| \log \pi_{\theta}(y_{w}^{i}|x^{i}) - |y_{l}^{i}| \log \pi_{\theta}(y_{l}^{i}|x)) \\ = & (\prod_{i=1}^{|B|} \exp(|y_{w}^{i}| \log \pi_{\theta}(y_{w}^{i}|x^{i}) - |y_{l}^{i}| \log \pi_{\theta}(y_{l}^{i}|x)))^{\frac{1}{|B|}} \\ = & (\prod_{i=1}^{|B|} \frac{\exp(-|y_{l}^{i}| \log \pi_{\theta}(y_{l}^{i}|x))}{\exp(-|y_{w}^{i}| \log \pi_{\theta}(y_{w}^{i}|x^{i}))})^{\frac{1}{|B|}} \\ = & (\prod_{i=1}^{|B|} \frac{\operatorname{PPL}(y_{l}^{i}|x)}{\operatorname{PPL}(y_{w}^{i}|x)})^{\frac{1}{|B|}} \\ = & G(\frac{\operatorname{PPL}(y_{l}|x)}{\operatorname{PPL}(y_{w}|x)}), \end{split}$$

which means that the exponential scaling function represents the geometric mean of the ratios of PPL for losing and winning responses within the training batch B, capturing their quality difference.

Finally, we have an intuitive understanding of Margin Scaling, which represents the quality gap between responses within the training batch.

$$h_{\gamma}(\gamma) = \beta G(\frac{\text{PPL}(y_l|x)}{\text{PPL}(y_w|x)})^{\alpha}.$$

D Experimental Details

D.1 Implementation Details

Overfitting-underfitting Problem Setups. To evaluate the Overfitting-underfitting Problem across offline preference optimization baselines (i.e. DPO and SimPO), we follow the methodology of (Lin et al. 2024; Hong et al. 2025), which evaluates ranking accuracy across the following four generalization scenarios based on prompt disjointness and response disjointness¹⁰.

Let $\mathcal{X}_{\text{train}} \subset \mathcal{X}$ and $\mathcal{X}_{\text{valid}} \subset \mathcal{X}$ be the sets of prompts used for generating responses in the training and validation sets respectively. $\mathcal{M}_{\text{train}} \subset \mathcal{M}$ and $\mathcal{M}_{\text{valid}} \subset \mathcal{M}$ represent the sets of models used for generating responses likewise. The corresponding response spaces are: $\mathcal{Y}_{\text{train}}(x) = \bigcup_{M_k \in \mathcal{M}_{\text{valid}}} \mathcal{Y}_k(x)$ and $\mathcal{Y}_{\text{valid}}(x) = \bigcup_{M_k \in \mathcal{M}_{\text{valid}}} \mathcal{Y}_k(x)$. Therefore, the training set for π_{θ} can be defined as follows:

$$\mathcal{D}_{\text{train}} = \{(x, y_w, y_l) \mid (y_w, y_l) \sim \mathcal{Y}_{\text{train}}(x), x \in \mathcal{X}_{\text{train}} \}.$$

In-Distribution (\mathcal{D}_{ID}). \mathcal{D}_{ID} samples from the seen prompt set \mathcal{X}_{train} and with the seen response model set \mathcal{M}_{train} .

$$\mathcal{D}_{\text{ID}} = \left\{ (x, y_w, y_l) \mid (y_w, y_l) \sim \mathcal{Y}_{\text{train}}(x), x \in \mathcal{X}_{\text{train}} \right\}.$$

Prompt-OOD ($\mathcal{D}_{\sim Prompt}$). $\mathcal{D}_{\sim Prompt}$ samples from the unseen prompt set $\mathcal{X}_{\text{valid}}$ but with the seen response model set $\mathcal{M}_{\text{valid}}$.

$$\mathcal{D}_{\sim \text{Prompt}} = \left\{ (x, y_w, y_l) \mid (y_w, y_l) \sim \mathcal{Y}_{\text{train}}(x), x \in \mathcal{X}_{\text{valid}} \right\}.$$

Response-OOD ($\mathcal{D}_{\sim Response}$). $\mathcal{D}_{\sim Response}$ samples from the seen prompt set \mathcal{X}_{train} but with the unseen response model set \mathcal{M}_{train} .

$$\mathcal{D}_{\sim \text{Response}} = \left\{ (x, y_w, y_l) \mid (y_w, y_l) \sim \mathcal{Y}_{\text{valid}}(x), x \in \mathcal{X}_{\text{train}} \right\}.$$

Mutual-OOD ($\mathcal{D}_{\sim Mutual}$). $\mathcal{D}_{\sim Mutual}$ samples from the unseen prompt set \mathcal{X}_{valid} and with the unseen response model set \mathcal{M}_{valid} .

$$\mathcal{D}_{\sim \text{Mutual}} = \{(x, y_w, y_l) \mid (y_w, y_l) \sim \mathcal{Y}_{\text{valid}}(x), x \in \mathcal{X}_{\text{valid}} \}.$$

For prompts with multiple responses (i.e. $\mathcal{D}_{\sim \text{Prompt}}$, $\mathcal{D}_{\sim \text{Response}}$ and $\mathcal{D}_{\sim \text{Mutual}}$), we select the highest-scoring one as chosen response y_w and the lowest-scoring one as rejected response y_l to evaluate ranking accuracy. In-distribution ranking accuracy on \mathcal{D}_{ID} demonstrates the learning capability of π_{θ} , measuring the underfitting. While out-of-distribution ranking accuracy on $\mathcal{D}_{\sim \text{Prompt}}$, $\mathcal{D}_{\sim \text{Response}}$ and $\mathcal{D}_{\sim \text{Mutual}}$ demonstrates the robustness of π_{θ} across generalization scenarios, measuring the overfitting. Therefore, we define the **Overfitting-underfitting Problem** as suboptimal in-distribution ranking accuracy and a degradation in out-of-distribution ranking accuracy.

Table 7: Searching ranges for hyperparameters across baseline

Method	Hyperparameter Search Range
DPO	$\beta \in [0.01, 0.05, 0.1]$
IPO	$\tau \in [0.01, 0.1, 0.5, 1.0]$
СРО	$\begin{array}{c} \lambda = 1.0 \\ \beta \in [0.01, 0.05, 0.1] \end{array}$
SLiC	$\begin{array}{l} \lambda \in [0.1, 0.5, 1.0, 10.0] \\ \delta \in [0.1, 0.5, 1.0, 2.0] \end{array}$
KTO	$\lambda_l = \lambda_w = 1.0$ $\beta \in [0.01, 0.05, 0.1]$
SimPO	$\beta \in [2.0, 2.5]$ $\gamma \in [0.3, 0.5, 1.0, 1.2, 1.4, 1.6]$
α-DPO	$\beta \in [2.5, 10.0], \gamma \in [0.1, 0.3, 0.5]$ $\alpha \in [1.0e-2, 5.0e-2, 0.1, 0.2]$
AMaPO	$\beta \in [1.0, 2.0, 3.0, 5.0]$

Training Hyperparameters. For general hyperparameters, we adhered strictly to the settings used in SimPO. We applied the following hyperparameters: For the SFT stage, we use a learning rate of 2×10^{-5} . For both the SFT and the preference optimization stages, we use a batch size of 128, a maximum sequence length of 2048 (1024 for Mistral-7B-Base setup), and a cosine learning rate schedule with 10% warmup steps for one epoch, all through the Adam optimizer (Kingma 2014). We maintain these settings consistently to ensure uniformity and comparability across experiments.

¹⁰https://huggingface.co/collections/rm-robustness

Table 8: Downstream tasks evaluation results on HuggingFace Open LLM Leaderboard

	Method	MMLU-PRO	IFEval	BBH	GPQA	MUSR	MATH	ARC	TruthfulQA	Winograd	Avg. Rank
	DPO	26.73	10.49	43.27	28.44	43.65	1.36	61.26	53.06	76.80	4.1
	SLiC	26.52	12.45	42.33	27.93	33.74	1.38	55.38	48.36	77.35	5.2
Mistral-7B	IPO	25.87	11.52	40.59	28.15	42.15	1.25	60.84	45.44	77.58	5.4
	KTO	27.51	12.03	43.66	29.45	43.17	2.34	62.37	56.60	77.27	2.5
Base	CPO	27.04	13.32	42.05	28.45	42.15	2.15	57.00	47.07	76.48	4.6
	SimPO	27.13	10.63	42.94	29.03	39.68	2.49	62.63	50.68	77.54	3.3
	AMaPO	27.52	10.45	44.70	31.70	42.20	1.30	62.54	52.87	78.37	2.8
	DPO	31.58	33.61	47.80	32.23	40.48	4.53	64.42	53.48	76.80	4.0
	SLiC	31.11	32.37	46.53	33.29	40.55	3.92	61.43	54.95	77.27	4.8
Llama3-8B	IPO	30.18	31.52	46.78	32.61	39.58	4.02	62.88	54.20	72.22	6.3
Base	KTO	31.16	37.10	47.98	33.72	40.21	4.14	63.14	55.76	76.09	3.8
Dase	CPO	30.95	38.57	47.17	33.15	41.59	4.25	61.69	54.29	76.16	3.9
	SimPO	31.61	37.55	48.38	33.22	40.08	4.23	65.19	59.46	76.32	2.8
	AMaPO	31.38	38.47	48.17	33.12	41.12	4.13	65.95	60.43	77.54	2.4
	DPO	26.81	22.89	45.46	28.19	46.43	1.89	66.89	68.40	76.32	3.6
	SLiC	25.69	29.53	45.24	27.04	43.90	1.95	59.90	65.30	76.32	5.7
Mistral-7B	IPO	25.75	27.85	43.81	26.61	43.55	2.02	63.31	67.36	75.85	6.0
Instruct	KTO	27.46	35.42	45.34	28.19	45.77	2.35	65.72	68.43	75.91	3.0
mstruct	CPO	26.85	36.81	45.01	28.15	43.28	2.28	63.23	67.38	76.80	4.3
	SimPO	27.10	37.52	45.70	28.04	44.71	2.19	66.89	68.40	76.32	2.9
	AMaPO	27.85	38.47	46.17	28.36	44.92	1.97	65.79	70.85	77.82	1.9
	DPO	35.86	44.57	48.31	31.04	39.02	8.23	63.99	59.01	74.66	2.3
	SLiC	33.25	44.01	47.55	30.52	38.10	8.29	61.26	53.23	76.16	4.7
Llama3-8B	IPO	32.97	43.27	46.31	30.95	38.58	8.02	61.95	54.64	73.09	5.6
Instruct	KTO	35.00	40.12	47.15	29.70	38.10	7.63	63.57	58.15	73.40	5.4
mstruct	CPO	34.56	44.08	48.51	30.08	38.81	7.75	62.29	54.01	73.72	4.6
	SimPO	35.09	43.05	48.95	31.29	39.15	8.16	62.80	60.70	73.32	3.1
	AMaPO	35.81	43.69	49.93	31.47	38.82	7.82	65.27	59.23	76.24	2.2

For method-specific hyperparameters, we also followed the search strategy from SimPO, noting that our method does not require any additional hyperparameters beyond the learning rate. Specifically, for different baseline methods, each with its own set of additional hyperparameters, the search strategy is in Table 7. Each method is individually searched for the learning rates in [4e-7, 6e-7, 8e-7, 1e-6].

Table 9: The hyperparameter value in AMaPo for each training setting

Setting	β	Learning rate
Llama3-8B-Base	3.0	6e-7
Llama3-8B-Instruct	3.0	1e-6
Mistral-7B-Base	2.0	4e-7
Mistral-7B-Instruct	2.0	6e-7

Hyperparameter in AMaPO. Table 9 outlines the hyperparameters used for AMaPo under various settings across experiments. Our method does not introduce any extra hyperparameter expect β inherited from the implicit reward function formulization. We have found through experience that β can be reliably set to around 2 by default. However, the learning rate typically requires more careful tuning, which can significantly influence the performance. We recommend a slightly larger learning rate setting than SimPO, where AMaPO only assigns an adaptive margin on a subset of samples, leading to a smaller but stable gradient norm.

Evaluation Hyperparameters. The hyperparameters for evaluation on AlpacaEval 2 adhere to SimPO, with a temperature of 0.7 for the Mistral-Base setting, a temperature of 0.5 for the Mistral-Instruct setting, and a temperature of 0.9 for both Llama3 settings. The hyperparameters for evaluation on MT-Bench are set according to the official decoding configuration, which specifies distinct sampling temperatures for various categories. We report the average MT-Bench score in 2 turns, and take the GPT-4-Preview-1106 as the judge model, which produces more accurate reference answers and judgments compared to GPT-4, with even lower cost (Meng, Xia, and Chen 2024).

Computation environent. All the training experiments in this paper were conducted on $4 \times$ NVIDIA A100 (80G) GPUs based on the alignment-handbook repo.

D.2 Preference Ranking across diverse domains

To thoroughly investigate the preference ranking gain of AMaPO, we report the RM-bench results across diverse domains, including Chat, Math, Code and Safety. As shown in Table 10, AMaPO consistently outperforms other baselines in various domains, especially in Chat and Safety domain. These significant improvements demonstrate that AMaPO is capable to generate more helpful and readable responses, which algins with our observations in AlpacaEval2 results in Table 2 and case study in Appendix E.

Table 10: RM-bench (Liu et al. 2024) results under the four setups, including Chat, Math, Code and Safety domains. Our AMaPO can achieve good performance on distinguishing responses across various setups.

(Method	Avg.	Chat	Math	Code	Safety
Mistral-7B Base	DPO SimPO α-DPO AMaPO	55.8 56.5 58.4 58.1	62.7 65.6 66.9 67.5	55.2 54.7 54.4 55.0	53.0 53.0 52.0 52.5	52.1 52.5 60.3 57.4
Llama3-8B Base	DPO SimPO α-DPO AMaPO	54.6 56.9 58.2 58.6	60.6 67.6 69.4 69.5	54.8 55.2 55.2 55.5	53.3 52.3 52.8 53.2	54.6 52.7 55.6 56.2
Mistral-7B Instruct	DPO SimPO α-DPO AMaPO	53.2 54.9 55.2 55.5	56.1 61.2 59.3 60.7	53.6 54.4 53.7 54.2	52.4 52.4 51.9 52.0	50.8 51.5 55.9 55.0
Llama3-8B Instruct	DPO SimPO α-DPO AMaPO	53.4 55.7 55.0 56.5	60.5 64.9 62.5 65.9	54.1 55.0 55.5 55.0	51.2 52.7 52.3 53.6	47.6 50.3 49.4 51.7

D.3 Downstream Task Evaluation

To further examine the performance of the policy model on downstream tasks across baselines, we also evaluate models fine-tuned with different methods on the same dataset across popular tasks listed on the Huggingface Open LLM Leaderboard v1 and v2¹¹ following previous works (Xiao et al. 2024, 2025). Open LLM Leaderboard encompasses ten tasks, including reasoning benchmarks (MMLU-PRO(Wang et al. 2024), Winogrande(Sakaguchi et al. 2021), ARC(Clark et al. 2018), IFEval(Zhou et al. 2023), BBH(Suzgun et al. 2022), GPQA(Rein et al. 2024)), mathematical reasoning (MATH(Hendrycks et al. 2021)), and safety benchmark (TruthfulQA(Lin, Hilton, and Evans 2021)). We follow the established evaluation protocols provided by the Language Model Evaluation Harness library(Gao et al. 2024) and present the results in Table 8.

Gain Significant improvements in Avg. rank. As shown in Avg. Rank column, AMaPo achieves the best performance across various downstream tasks and setups mostly. These consistent and significant improvements highlight the robustness and effectiveness of our method, which suggest that enhanced preference ranking capabilities can help the policy model complete downstream tasks.

Reading comprehension and commonsense reasoning improve. For ARC and Winograd, which require strong comprehension and reasoning capabilities, AMaPO achieves remarkable improvements over baselines. We hypothesis that our method helps the policy model to capture and understand the subtle differences in responses, aligning with the observations on RM-Bench (see Table 3), then generalize to better reasoning performance.

Math performance drops. However, although a significant improvement of AMaPO is observed on the ranking accuracy in code and math domain, AMaPO still exhibits a huge drop in MATH. We hypothesize that there is a gap

between identifying and generating an accurate response. Specifically, AMaPO consistently underperforms SimPO in MATH, which suggests that assigning a positive margin for correctly ranked samples may help the generation performance on math tasks. These findings emphasize the importance of the margin design, and further exploration is left to future work.

Table 11: Ablation study of oracle margin estimation under Llama3-8B-Base setup.

Batch	RM-	Bench	Alpac	aEval2
Size	Easy (%)	Hard (%)	LC (%)	WR (%)
16	88.2	24.5	27.9	23.5
32 (default)	87.8	25.4	26.4	21.4
64	87.5	25.8	22.1	20.8

D.4 Ablation Study of Oracle Margin Estimation

To validate the robustness of our proposed estimation methods based on the mean implicit reward margin within the batch, we conduct ablation study towards the batch size hyperparameter. To ensure a fair comparison, we adjusted the batch size for oracle margin estimation while holding the total number of gradient update steps constant (the same as default setup) for under Llama3-8B-Base setup on Ultrafeedback Binarized dataset. As shown in Table 11, results on ranking accuracy and downstream generation benchmarks, demonstrate the robustness of our oracle margin estimation. Specifically, an increasing batch size leads to a performance drop on the RM-Bench Easy accuracy but a gain on the Hard accuracy. This implies that AMaPO amplifies the gradients for hard, incorrectly ranked samples, demonstrating that a larger batch size facilitates a more precise estimation of the oracle margin. However, results on AlpacaEval2 show an opposite trend. This is consistent with our ablation studies over β in Section 5.3, which indicates that excessively amplifying the gradients of hard samples leads to distribution sharpening, resulting in a degradation of downstream performance. Our analysis reveals that AMaPO not only consistently outperforms strong baselines (Table 2) irrespective of the batch size, but its performance sensitivity across diverse datasets also provides compelling empirical evidence for the two limiting cases predicted by our theory, thereby validating both the practical effectiveness and theoretical soundness of our approach.

D.5 Reward Distribution of Different Models

To validate that a tuned policy model is a better option to estimate the oracle reward margin, we visualize the distribution of reward margin on Ultrafeedback Binarized dataset under Llama3-Base-8B setup with popular methods (i.e. DPO and SimPO). As shown in Figure 2, tuned policy models, SimPO specifically, exhibit a rightward skew distribution with a larger variance, suggesting that tuned policy models are more likely to produce accurate oracle reward margin.

¹¹ https://huggingface.co/open-llm-leaderboard

Table 12: Detailed results of ablation studies on AlpacaEval2.

Method		Llama3	-8B-Base		Llama3-8B-Instruct			
	LC (%)	WR (%)	STD (%)	Length	LC (%)	WR (%)	STD (%)	Length
AMaPO	26.4	21.4	1.3	1592	46.1	41.3	1.5	1776
w/o Z-norm w/o exp w/o adaptive w/o zero	24.8 24.0 20.7 22.3	20.4 17.6 16.4 21.1	1.4 1.2 1.1 1.3	1754 1480 1493 1918	44.2 47.1 47.2 48.6	39.6 42.9 42.5 45.0	1.6 1.6 1.6 1.6	1754 1783 1790 1828

Table 13: Detailed results of AlpacaEval2. LC means length-controlled win tate, WR means raw win rate, and STD means standard deviation of win rate. Length is the average generation length.

Method		Llama3	-8B-Base		Llama3-8B-Instruct				
	LC (%)	WR (%)	STD (%)	Length	LC (%)	WR (%)	STD (%)	Length	
SFT	6.2	4.6	0.7	1082	26.0	25.3	1.3	1920	
DPO	18.2	15.5	1.1	1585	40.3	37.9	1.4	1883	
SLiC	12.3	13.7	0.9	1540	26.9	27.5	1.3	1977	
IPO	14.4	14.2	1.1	1856	35.6	35.6	1.4	1983	
KTO	14.2	12.4	1.0	1646	33.1	31.8	1.4	1909	
CPO	10.8	8.1	1.0	2495	28.9	32.2	1.4	2166	
SimPO	22.0	20.3	1.2	1795	44.7	40.5	1.4	1825	
α -DPO	21.7	20.6	1.3	1913	46.6	39.6	1.6	1759	
AMaPO	26.4	21.4	1.3	1592	46.1	41.3	1.5	1776	
Method		Mistral-	-7B-Base		Mistral-7B-Instruct				
	LC (%)	WR (%)	STD (%)	Length	LC (%)	WR (%)	STD (%)	Length	
SFT	8.4	6.2	1.1	914	17.1	14.7	1.1	1676	
DPO	15.1	12.5	1.0	1477	26.8	24.9	1.3	1808	
SLiC	10.9	8.9	0.9	1525	24.1	24.6	1.3	2088	
IPO	11.8	9.4	0.9	1380	20.3	20.3	1.2	2024	
KTO	13.1	9.1	0.9	1144	24.5	23.6	1.3	1901	
CPO	9.8	8.9	0.9	1827	23.8	28.8	1.3	3245	

1868

1200

1700

32.1

34.2

34.5

34.8

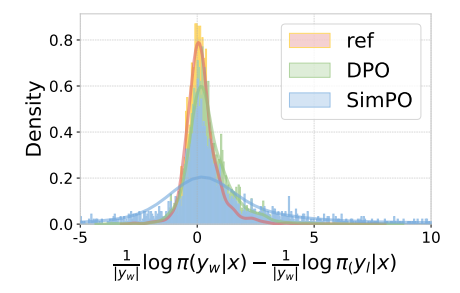
33.8

35.1

1.4

1.6

1.5



SimPO

 α -DPO

AMaPO

21.5

17.2

24.3

20.8

13.0

20.6

1.2

1.1

1.3

Figure 2: Reward margin on the test set of Ultrafeedback Binarized.

D.6 Generation Length Analysis

AMaPO decreases generation length and improves generation quality. As we have observed that AMaPO exhibits a significant on AlpacaEval2 LC win rate improvement compared to other baselines, to further analyze the underlying working inners, we first report the detailed results of AlpacaEval2 including the strandard deviation and generation length. As shown in Table 13, although AMaPO outperforms

baselines on WR slightly, it generates response extremely shorter than comparable baselines. Notably, AMaPO decreases the generation length by up to 203 tokens compared to SimPO. This suggests that AMaPO can effectively control the verbosity of the generated responses, and meanwhile improve the generation quality to a certain extent. Also, we find that the designs of adaptive margin profoundly impact the generation length, as shown in Table 12. Specifically, removing the zero setting for correctly ranked samples increases the generation length significantly. We argue that it is caused by learning the preference patterns from the already correctly ranked samples, in which preferred responses tend to be longer in existing preference datasets.

2193

1980

2121

E Case Study

In this section, we present examples where Llama-Instruct-AMaPO generates a better-structured answers compared to Llama-Instruct-SimPO in AlpacaEval2 benchmark.

Given the question, "What are the names of some famous actors that started their careers on Broadway?", the SimPO model generates a response that only contains a list of celebrity names, lacking corresponding explanatory material. In contrast, the AMaPO model produces a detailed

answer that not only lists celebrity names but also covers their famous acting experiences. This helps users learn about celebrities faster and makes it easier to verify the information's authenticity, indicating that AMaPO can better leverage its internal knowledge.

Similarly, given the question, "How to improve instance segmentation AP metrics with human knowledge", the SimPO model generates a response with a long list of bullet points, making it difficult to understand the relationships between different points. In contrast, the AMaPO model produces a well-structured answer with high-level categorization of different behaviors, organized with a General-Specific-General structure with the markdown form. This makes the answer more readable and easier to understand.

- **AMaPO** Many talented actors have transitioned from Broadway to Hollywood success. Here are some famous examples:
 - 1. Julie Andrews: Starred in Broadway's "My Fair Lady" (1956) and Camelot (1960) before becoming a movie icon in films like The Sound of Music (1965) and Mary Poppins (1964).
 - 2. Hugh Jackman: Originated the role of Curly in Broadway's Oklahoma! (1998) and later starred in films like X-Men (2000), Les Misérables (2012), and The Greatest Showman (2017).
 - 3. Neil Patrick Harris: Got his start on Broadway in Assassins (1990) and Rent (1996) before becoming a TV star in Doogie Howser, M.D. and later How I Met Your Mother.
 - 4. Idina Menzel: Originated the role of Maureen Johnson in Broadway's Rent (1996) and later voiced Elsa in Disney's Frozen (2013) and starred in TV's Glee.
 - 5. Lin-Manuel Miranda: Created and starred in Broadway's In the Heights (2008) and Hamilton (2015), earning multiple Tony Awards and a film career in Moana (2016) and Mary Poppins Returns (2018).
 - 6. Nathan Lane: Began his career on Broadway in Noises Off (1983) and Guys and Dolls (1992), later appearing in films like The Birdcage (1996) and TV's Modern Family.
 - 7. Bernadette Peters: Starred in Broadway's Song and Dance (1985) and Into the Woods (1987), with notable film roles in The Muppet Movie (1979) and TV's Smach
 - 8. Alan Cumming: Originated the role of Emcee in Broadway's Cabaret (1998) and has since appeared in films like X2: X-Men United (2003), Spy Kids (2001), and TV's The Good Wife.
 - 9. Sutton Foster: Got her start on Broadway in Annie (1997) and Thoroughly Modern Millie (2002), later starring in TV's Bunheads and Younger.
 - 10. Laura Linney: Began her career on Broadway in Six Degrees of Separation (1990) and The Little Foxes (1997), with notable film roles in The Truman Show (1998) and TV's Ozark.

These are just a few examples of talented actors who started their careers on Broadway and went on to achieve success in film and television.

SimPO 1. Hugh Jackman

- 2. Audra McDonald
- 3. Bernadette Peters
- 4. Angela Lansbury
- 5. Meryl Streep
- 6. Matthew Broderick
- 7. Nathan Lane
- 8. Patti LuPone
- 9. Lin-Manuel Miranda
- 10. Glenn Close
- 11. Cynthia Nixon
- 12. Liev Schreiber
- 13. Sutton Foster
- 14. James Earl Jones
- 15. Phylicia Rashad
- 16. Leslie Odom Jr.
- 17. Jessie Mueller
- 18. Kelli O'Hara
- 19. Brian Stokes Mitchell
- 20. Bernadette Peters (again, as mentioned earlier)",

Table 14: An AlpacaEval 2 generation from the Llama-3-8B-Instruct model trained with AMaPO and SimPO. Weighted-Alpaca-Eval-GPT4-Turbo prefers AMaPO over SimPO. Compared to SimPO, the generation by AMaPO contains more related information, with hierarchical discussions that make it more helpful.

Prompt How to improve instance segmentation AP metrics with human knowledge

- AMaPO Instance segmentation models, such as Mask R-CNN, typically evaluate their performance using metrics like Average Precision (AP) and Intersection over Union (IoU). While these metrics provide a quantitative measure of performance, incorporating human knowledge can help improve instance segmentation models in several ways:
 - 1. **Annotate challenging cases**: Identify and annotate instances with complex or ambiguous boundaries, occlusions, or unusual appearances. This helps the model learn to handle these edge cases better.
 - 2. **Provide domain-specific knowledge**: Incorporate domain expertise into the annotation process by highlighting important features, such as texture, color, or shape, that are relevant to the specific application (e.g., medical imaging, autonomous driving).
 - 3. **Use weak supervision**: Instead of annotating every instance, use weak supervision techniques like:
 - Bounding box annotations: Provide approximate bounding boxes around instances, allowing the model to learn from rough estimates.
 - Semantic segmentation masks: Annotate classes or categories, rather than individual instances, to help the model understand the context and relationships between objects.
 - 4. **Regularly update and refine annotations**: As the model improves, revisit and refine the annotations to ensure they remain accurate and relevant. This helps the model adapt to its own mistakes and learn from corrections.
 - 5. Use transfer learning and multi-task learning: Initialize the model with pretrained weights on a related task or dataset, and then fine-tune it on your specific instance segmentation task. This can leverage knowledge from other domains or tasks to improve performance.
 - 6. **Incorporate prior knowledge into the model architecture**: Design the model to incorporate domain-specific constraints or features, such as:
 - Using attention mechanisms to focus on relevant regions or features.
 - Incorporating shape priors or geometric constraints to improve instance segmentation.
 - 7. **Use human-in-the-loop evaluation**: Involve human evaluators in the evaluation process to:
 - Provide feedback on model performance and identify areas for improvement.
 - Correct mistakes and annotate challenging cases.

leading to better AP metrics and more accurate results.

- Validate the model's output and ensure it aligns with human expectations.

Explore alternative evaluation metrics: Consider using metrics that better capture the nuances of instance segmentation, such as:

- Instance-level metrics like mean Average Precision (mAP) or mean Average Recall (mAR).
- Metrics that account for instance size, orientation, or aspect ratio.
- 9. **Regularly monitor and analyze model behavior**: Use visualization tools and techniques to understand how the model is making predictions, identifying biases, and areas where it struggles. This helps you to refine the model and annotations accordingly.
- 10. **Collaborate with domain experts**: Work closely with experts in the domain to ensure the model is aligned with their understanding of the problem and to incorporate their insights into the annotation process and model development. By incorporating these strategies, you can leverage human knowledge to improve the performance and robustness of your instance segmentation model, ultimately

- **SimPO** 1. **Incorporate Prior Knowledge**: Incorporating domain-specific knowledge, such as object categories, shapes, textures, and common configurations, can enhance instance segmentation models' performance. For instance, leveraging preexisting object detection models or semantic segmentation models can provide additional context and guidance for instance segmentation.
 - 2. Collaborative Learning: Collaborative learning involves incorporating human feedback into the training process. This approach involves collecting annotations from human experts, such as bounding boxes or segmentation masks, for a subset of images, and using them to guide the model's learning process. This feedback can help the model better understand object boundaries, relationships, and nuances, leading to improved segmentation accuracy.
 - 3. **Active Learning**: Active learning involves selecting the most informative samples for annotation based on the model's uncertainty or confidence scores. By prioritizing challenging instances, human annotators can focus their efforts on areas where the model struggles, leading to more targeted feedback and improved instance segmentation performance.
 - 4. **Multi-Task Learning**: Combining instance segmentation with other relevant tasks, such as object detection, semantic segmentation, or panoptic segmentation, can leverage shared features and enhance the model's overall understanding of the scene. This approach can improve the segmentation accuracy by providing additional supervision signals and reducing the semantic gap between different tasks.
 - 5. **Domain Adaptation**: Instance segmentation models trained on synthetic datasets or generic benchmarks may not generalize well to real-world scenarios with varying backgrounds, lighting conditions, and object appearances. Incorporating domain-specific knowledge, such as transfer learning from pre-trained models, data augmentation techniques, or adversarial training, can help adapt the model to specific domains, leading to better instance segmentation performance.
 - 6. **Ensemble Methods**: Combining multiple instance segmentation models with diverse architectures, training strategies, or loss functions can leverage their strengths and mitigate their weaknesses, resulting in improved overall performance. Ensemble methods, such as voting or weighted averaging, can aggregate predictions from multiple models, reducing uncertainty and increasing robustness.
 - 7. **Post-Processing Techniques**: Applying post-processing techniques, such as non-maximum suppression, merging overlapping segments, or refining segmentation masks based on contextual cues, can enhance the segmentation quality and reduce false positivesnegatives. Human knowledge can guide the selection of appropriate thresholds, heuristics, or priors for these techniques, leading to more accurate instance segmentation results.
 - 8. **Interactive Feedback Loops**: Interactive feedback loops involve iteratively refining the segmentation results with human feedback, allowing for continuous improvement and adaptation. This approach involves presenting segmentation outputs to human annotators, soliciting feedback, and incorporating it back into the model's training pipeline. This iterative process can lead to more accurate segmentation results tailored to specific use cases or applications.

Table 15: An AlpacaEval 2 generation from the Llama-3-8B-Instruct model trained with AMaPO and SimPO. Weighted-Alpaca-Eval-GPT4-Turbo prefers AMaPO over SimPO. Compared to SimPO, the generation by AMaPO is organized with a General-Specific-General structure, with markdown form makes it easier to read.